EUROPEAN COMMISSION
European Research Area

Karlsruhe Institute of Technology

Large Scale Experiments on Core Degradation, Melt Retention and Containment Behaviour (LACOMECO Project)

Grant Agreement Number: 249682

FINAL REPORT

A. Miassoedov[1], G. Albrecht[1], H. Combeau[4], B. Fluhrer[1], X. Gaus-Liu[1], M. Große[1], J. Grune[7], Z. Hózer[2], I. Kljenak[8], F. Kretzschmar[1], S. Kudriakov[3], M. Kuznetsov[1], M. Matkovič[8], B. Mavko[8], R. Meignen[5], R. Porowski[6], G. Ratel[3], B. Raverdy[5], W. Rudy[6], J. M. Seiler[3], K. Sempert[7], M. Steinbrück[1], J. Stuckert[1], E. Studer[3], A. Teodorczyk[6]

[1]KIT, Karlsruhe, Germany
[2]MTA Centre for Energy Research, Budapest, Hungary
[3]CEA, France
[4]Institut Jean Lamour, Lorraine University, Nancy, France
[5]IRSN, Fontenay aux Roses, France
[6]Warsaw University of Technology, Poland
[7]Pro-Science GmbH, Karlsruhe, Germany
[8]Jozef Stefan Institute, Ljubljana, Slovenia

Project co-funded by the European Commission within the 7th Framework Programme (2007-2013)		
Dissemination Level		
PU	Public	**PU**
RE	Restricted to a group specified by the LACOMECO partners	
CO	Confidential, only for LACOMECO partners	
CR	Confidential, only for LACOMECO partners working on the same subject	

Date of issue: 02/09/2013

TABLE OF CONTENTS

LIST OF TABLES

LIST OF FIGURES

1 Executive summary

The objective of the LACOMECO project is to offer EU research institutions access to four experimental facilities QUENCH, LIVE, DISCO and HYKA at Karlsruhe Institute of Technology (KIT) which are designed to study the remaining severe accident safety issues, ranked with high or medium priority by the SARNET Severe Accident Research Priorities (SARP) group for SARNET. These issues are coolability of a degraded core, corium coolability in the RPV, possible melt dispersion to the reactor cavity, and hydrogen mixing and combustion in the containment. These facilities are unique, without rival in other Member States and therefore could be used for experimental programmes in specific fields of core damage initiation up to hydrogen behaviour.

The access to LACOMECO was widely published, so that the researchers throughout the Member States of the Community and the FP7 Associated States were made aware of the possibilities open to them. As a result of the call for proposals seven proposals had been received, of which 2 were for QUENCH, 1 for LIVE, 1 for DISCO and 3 for HYKA. As a result of the evaluation 1 experiment was selected for QUENCH, 1 for LIVE, 1 for DISCO and 2 for HYKA. Due to the great interest of the User Selection Panel for all 3 proposals for HYKA, it was proposed by KIT to perform all three tests. Following tests have been performed within the LACOMECO project in cooperation with partners from different countries like Hungary, France, Poland and Slovenia:

- QUENCH test with slow oxidation in air (QUENCH-16)
- LIVE test to examine the dissolution kinetics of a pure KNO_3 crust by a $KNO_3/NaNO_3$ melt (LIVE-CERAM)
- DISCO test related to ex-vessel fuel coolant interaction (DISCO-FCI)
- HYKA tests to investigate detonations in partially confined layers of hydrogen-air mixtures (DETHYD)
- HYKA tests related to hydrogen concentration gradients effects understanding and modelling (HYGRADE)
- HYKA test to investigate upward flame propagation in air-steam-hydrogen atmosphere (UFPA)

For the preparation of the tests and for the definition of the experimental conditions, intensive discussions between the partners took place via email exchange and during separate partner meetings or meetings of other European projects, like SARNET Review Meetings and Quench workshop.

The results of the experiments performed under the LACOMECO project are distributed to the SARNET2 community and are used for the development of models and their implementation in the severe accident codes such as ASTEC. This will help to capitalise the knowledge obtained in the field of severe accident research in the ASTEC code and the scientific databases, thus preserving and disseminating this knowledge to a large number of current and future end-users throughout Europe. Moreover, the knowledge obtained in the project shall lead to improved severe accident management measures, which are essential for reactor safety and in addition offer competitive advantages for the European industry.

The project brought together competent teams from different countries with complementary knowledge. Moreover, the links with the East European research organisations and utilities was established and maintained. Therefore, the project offered a unique opportunity to join networks and activities supporting VVER safety, and for Eastern experts to get access to large scale experimental facilities in a Western research organisation, thereby improving

the understanding of material properties, core behaviour, and containment safety under severe accident conditions.

2 Summary description of project context and objectives

The objective of the LACOMECO project is to offer EU research institutions access to four experimental facilities QUENCH, LIVE, DISCO and HYKA at Karlsruhe Institute of Technology (KIT) which are designed to study the remaining severe accident safety issues, ranked with high or medium priority by the SARNET Severe Accident Research Priorities (SARP) group for SARNET. These issues are coolability of a degraded core, corium coolability in the RPV, possible melt dispersion to the reactor cavity, and hydrogen mixing and combustion in the containment. These facilities are unique, without rival in other Member States and therefore could be used for experimental programmes in specific fields of core damage initiation up to hydrogen behaviour. In addition, the experiments performed in the project are designed to be complementary to other European facilities and experimental platforms to form a coherent European nuclear experimental network.

Severe accidents can cause significant damage to reactor fuel resulting in more or less complete core meltdown and threaten the containment integrity. Such accidents are highly unlikely in light of the preventive measures implemented by operators. However, they are the focus of considerable research, because the release of radioactive products into the environment would have serious consequences. This research also reflects a commitment to the defence-in-depth approach.

As stated in the final draft of the Strategic Research Agenda (SRA) of the Sustainable Nuclear Energy Technology Platform (SNETP), needs for safety research are identified by both regulators and operators, from their respective perspective. As discussed in the SRA, safety research is still needed to support long-term operation of existing LWRs in Europe. Though the SRA cannot integrate all national programmes on safety research carried out in Europe, the platform members agree on the issues that are of highest priority. Regarding the issues in severe accidents, the SRA refers to the work carried out in the framework of the Severe Accident Research Network of Excellence (SARNET) to conclude to a common view on the ranking of the research priorities in the field. The research priorities on severe accident management were prepared and are being continuously reviewed and updated by the SARNET SARP group. The objective of the group is to review and reassess the priorities of research issues and to propose the results as basis to harmonise and to re-orient research programmes, to define new ones, and to close – if possible – resolved issues on a common basis.
After two years of intense discussions and three meetings of the SARP group, the R&D priorities on severe accident management are ranked in 4 groups:

1. Six issues are regarded to be investigated further with high priority (further research is considered as necessary):
   - Core coolability during reflood and debris cooling;
   - Ex-vessel melt pool configuration during Molten Corium Concrete Interaction (MCCI), ex-vessel corium coolability by top flooding;
   - Melt relocation into water, ex-vessel Fuel Coolant Interaction (FCI);
   - Hydrogen mixing and combustion in containment;
   - Oxidising impact (Ruthenium oxidising conditions/air ingress for High Burn-up and Mixed Oxide fuel elements) on source term;
   - Iodine chemistry in Reactor Coolant System (RCS) and in containment.

2. Four issues are re-assessed with medium priority (these items should be investigated further as already planned in the different research programs):
- Hydrogen generation during reflood and melt relocation in vessel;
- Corium coolability in lower head;
- Integrity of Reactor Pressure Vessel (RPV) due to external vessel cooling;
- Direct containment heating (DCH).

3. Five issues are assessed with low priority (could be closed after the related activities are finished):
- Corium coolability in core catcher with external cooling;
- Corium release following vessel rupture;
- Crack formation and leakages in concrete containment;
- Aerosol behaviour impact on source term (in steam generator tubes (SGT) and containment cracks);
- Core reflooding impact on source term.

4. Three issues could be closed because of low risk significance and sufficient current state of knowledge:
- Integrity of reactor coolant system and heat distribution;
- Ex-vessel core catcher and corium-ceramics interaction, cooling with water bottom injection;
- FCI including steam explosion in weakened vessel.

The phenomena described above are extremely complex; they generally demand the development of specific research. This research involves very substantial human and financial resources and, in general, the research field is too wide to allow investigation of all phenomena by any national programme. To optimise the use of the resources, the collaboration between nuclear utilities, industry groups, research centres and safety authorities, at both national and international levels is very important. This is precisely the main objective of the LACOMECO project, which aims to provide these resources and to facilitate this collaboration by offering four large scale experimental facilities at the Karlsruhe Institute of Technology (KIT) for transnational access. The LACOMECO experimental platform at KIT includes:

- **QUENCH** facility is the only operating experimental facility within the European Union for investigations of the early and late phases of core degradation in prototypic geometry for different reactor designs and different cladding alloys, incl. analysis of the relocation of cladding and fuel and the formation and cooling of in-core debris beds to gain information on the characteristics of the created particles.
- **LIVE** facility concentrates on the investigation of the whole evolution of the in-vessel late phase of a severe accident, including e.g. formation and growth of the in-core melt pool, characteristics of corium arrival in the lower head, and molten pool behaviour after the debris re-melting in large scale 3D geometry with emphasis on the transient behaviour.
- **HYKA** experimental facilities are among the largest available in the world. In combination with the high static and dynamic pressures the experimental facilities are designed for, a unique experimental centre especially for combustion experiments in confined spaces is available with HYKA. Due to the different orientations and sizes the set of large and strong experimental vessels offers a flexible basis for scientific experimental work on reactive hydrogen mixtures.

- **DISCO** is the only operating facility available worldwide for integral Direct Containment Heating (DCH) investigations. It is designed to perform scaled experiments that simulate melt ejection from the RPV to the reactor cavity after the RPV failure under low system pressure during severe accidents in LWRs. These experiments investigate the fluid-dynamic, thermal and chemical processes during melt ejection out of a breach in the lower head of an LWR pressure vessel at pressures below 2 MPa.

The overall purpose of these test facilities is to investigate core melt scenarios from the beginning of core degradation to melt formation and relocation in the vessel, possible melt dispersion to the reactor cavity and to the containment, and finally hydrogen-related phenomena in severe accidents. The use of these facilities will provide the interested partners of the European Member Countries and FP7 Associated States a focus on core quenching, on possible core melt sequences in the RPV, on melt dispersion and on hydrogen behaviour in the containment, to enhance the understanding of severe accident sequences and their control in order to increase the public confidence in the use of nuclear energy.

The main thrust of this project is towards large scale tests under prototypical conditions. These will help the understanding of core degradation and quenching, melt formation and relocation as well as core coolability in real reactors in two ways – firstly by scaling-up and secondly by providing data for the improvement and validation of computer codes applied for safety assessment and planning of accident mitigation concepts, such as ASTEC.

The importance of the LACOMECO project for the European research is reflected in three aspects:

1) The access to large scale experimental facilities is proposed to investigate all important processes from the early core degradation to late in-vessel phase pool formation in the lower head, continuation to ex-vessel melt situations and to the hydrogen behaviour in the containment. Therefore two high priority and three medium priority issues identified by the SARP group will be addressed in the project, namely
   - Core coolability during reflood and debris cooling (high);
   - Hydrogen mixing and combustion in containment (high);
   - Hydrogen generation during reflood and melt relocation in vessel (medium);
   - Corium coolability in lower head (medium);
   - Direct containment heating (medium).
2) The results of the project will be applicable to the European reactor fleet taking into account the main light water reactors including Eastern ones (VVER design). A European vision is used to decide priorities in the experimental programme.
3) The project offers a unique opportunity for Eastern experts to get an access to large scale facilities in Western research organisation to improve understanding of material properties and core behaviour under severe accident conditions, and to become familiar with the high level safety concepts in nuclear power plants.

Specifically, the access to LACOMECO platform shall provide answers to the following questions:

1) QUENCH: What are the main factors governing the hydrogen source term, formation and coolability of corium debris and melt behaviour during core quenching?
2) LIVE: What will be the time span of melt relocation to the lower plenum, what are the main phenomena governing the corium debris bed formation and what measures are needed to regain the in-vessel debris and core melt coolability?

3) DISCO: Where will the melt be located after failure of the RPV under moderate pressure, with different RPV failure modes? What is the pressure increase in the reactor pit, the sub-compartments and the containment due to thermal and chemical reactions (hydrogen production and burning)?
4) HYKA: Is the experimental and theoretical basis of predicting the turbulent combustion, flame acceleration and detonation onset in hydrogen/air mixtures sound enough and how can the hydrogen mitigation measures be improved?

To answer these questions the LACOMECO project has:
1) planned and carried out one experiment in the QUENCH facility that simulates as closely as possible key scenarios of a reactor core degradation for main classes of European light water reactors;
2) conducted one experiment in 1:5 scaled RPV geometry in the LIVE facility with different melt masses and relocation modes to study debris remelting and cooling mechanisms, to quantify heat flux distribution, crust formation and stability, and possible cooling modes;
3) performed one experiment in a scaled reactor geometry in the DISCO facility at prototypical pressures and temperatures to simulate melt dispersion in the containment after the RPV failure;
4) performed three experiments in the HYKA facility to investigate the hydrogen-related phenomena in severe accidents, including hydrogen distribution, hydrogen combustion and hydrogen mitigation measures.

SARP issues, which are addressed in the LACOMECO project, are:
- Core coolability during reflood and debris cooling;
- Melt relocation into water, ex-vessel Fuel Coolant Interaction;
- Hydrogen mixing and combustion in containment;
- Hydrogen generation during reflood and melt relocation in vessel;
- Corium coolability in lower head.

At present, knowledge of various core melt sequences and the consequences of possible operator actions are not yet sufficient as they are too dependent on specific characteristics of the power plant under consideration. LACOMECO aims to provide the resources for a better understanding of possible scenarios of core quenching, different core melt sequences and hydrogen behaviour for different reactor designs. This knowledge shall lead to improved severe accident management measures, which are essential for reactor safety and in addition offer competitive advantages for the European industry.

The results of the experiments performed under the LACOMECO project were distributed to the SARNET2 community and will be used for the development of models and their implementation in the severe accident codes such as ASTEC. This will help to capitalise the knowledge obtained in the field of severe accident research in the ASTEC code and the scientific databases, thus preserving and diffusing this knowledge to a large number of current and future end-users throughout Europe.

One of the main achievements of the SARNET NoE was the review and reassessment of the priorities on severe accident research issues on which research was still considered as necessary. The activities within the LACOMECO project will allow advancing considerably towards understanding and perhaps evening closure of these issues. It will thereby optimise

the resources (both available expertise and experimental facilities) to focus on these issues given the reduction of national budgets.

The project brought together competent teams from different countries with complementary knowledge. Moreover, the links with the East European research organisations and utilities was established and maintained. Therefore, the project offered a unique opportunity to join networks and activities supporting VVER safety, and for Eastern experts to get access to large scale experimental facilities in a Western research organisation. They thereby improved their understanding of material properties, core behaviour, and containment safety under severe accident conditions.

3 Description of the main S&T results/foregrounds

The LACOMECO project was structured in 5 work packages. The main S&T results for each work package are summarised in the following sections.

3.1 WP0 MANAG

This work package covers all administrative, legal and financial issues.

At the beginning of the project, the project Executive Group widely published the access to LACOMECO, so that the researchers throughout the Member States of the Community and the FP7 Associated States were made aware of the possibilities open to them. Call for proposals with deadline of 30 April 2010 was advertised on a dedicated website on the internet and information about the call for proposals was distributed at international conferences and through emails. New Member Countries were particularly encouraged to participate. As a result of the call for proposals seven proposals had been received. The proposals were distributed in the relevant SARNET2 work packages for comments, improvements and recommendations on experiment performance. Following the SARNET review, LACOMECO User Selection Panel meeting was held on July 8, 2010 in Bratislava. The objective was to prepare recommendations to the European Commission regarding selection of experiments to be performed in the QUENCH, LIVE, DISCO, and HYKA facilities, arising from the first call of proposals. From the seven proposals, 2 were for QUENCH, 1 for LIVE, 1 for DISCO and 3 for HYKA. One test was to be selected for QUENCH, LIVE, and DISCO and up to 2 for HYKA. The decision process involved presentation of the proposals by the responsible person at KIT, indicating for example the complexity, benefit and risk of each, followed by a group discussion. As a result of the evaluation 1 experiment was selected for QUENCH, 1 for LIVE, 1 for DISCO and 2 for HYKA. Due to the great interest of the User Selection Panel for all 3 proposals for HYKA, it was proposed by KIT to perform all three proposed tests.

During the LACOMECO project several project meetings were organised. Furthermore, intensive discussions of the test preparation and experimental conditions between the partners involved in different experiments continuously took place via email exchange and during meetings of other European projects, like SARNET Review Meetings, Quench Workshop, etc.
For the planning and conduction of the different experiments in total 11 researchers from the different partners visited the test facilities at KIT.

Co-operation with other projects has been established, e.g. between LACOMECO and SARNET2 projects. Links between the LACOMECO project and PLINIUS severe accident

platform of CEA Cadarache were also established. A first joint workshop was held in October 2010 in Aix-en-Provence (FR).

3.2 WP1 QUENCH

Core coolability during reflood and corium debris cooling as well as in-vessel hydrogen generation during reflood and core melt relocation are ranked as *high and medium priority issues by the SARP group of the SARNET NoE*. Bundle experiments in the QUENCH facility are specifically designed to contribute to the reduction in uncertainties and increase in understanding of these issues. This is necessary to reach a proper assessment of the risk posed by quenching of degraded core to full-scale power plants.

The QUENCH program aims not only to determine the amount of hydrogen released during reflood of a test bundle with genuine core materials as cladding and spacer grids, but also to investigate the related high-temperature interactions of the core materials. The QUENCH bundle experiments are supported by an extensive separate-effects test programme which is performed to generate comprehensive data for model development and subsequent implementation into SFD computer codes.

The QUENCH test facility can be operated in two modes: (a) a forced-convection mode with a flow of ~3 g/s of superheated steam of ~600 °C together with argon and (b) a boil-off mode with the steam inlet line closed. The system pressure in the test section is usually around 0.2 MPa (max. 0.6 MPa). Quenching can be performed with water or saturated steam from the bottom. Top quenching is prepared in the design of the facility but has not yet been realised.

The main component is the test bundle that can be a standard PWR or e.g. a VVER -type. The PWR-type test bundle with a pitch of 14.3 mm is made up of 21 fuel rod simulators with Zircaloy-4 rod claddings and spacer grids whereas a VVER-type bundle consists of 31 rods arranged in a hexagonal lattice with a pitch of 12.75 mm. The VVER claddings and spacer grids are made of Zr1%Nb. Each bundle has a total length of approximately 2.5 m with a heating length of approximately 1 m. Heating is electric by tungsten heaters installed in the rod centre and surrounded by annular ZrO_2 pellets. Electrodes of molybdenum and copper connect the heaters with the cables leading to the DC electric power supply capable of 70 kW. The central rod is unheated and used for instrumentation or as absorber rod, e.g. B_4C or Ag-In-Cd to study their influence on core degradation. The test bundle is surrounded by a 2.38 mm thick shroud of Zircaloy together with a 37 mm thick ZrO_2 fibre insulation that extends to the upper end of the heated zone and a double-walled cooling jacket of stainless steel/Inconel. Corner rods are inserted in the bundle to adapt the bundle hydraulic diameter. These rods made of the same material as the rod claddings are either used for thermocouple instrumentation or as probe which can be withdrawn from the bundle anytime during the test to check the degree of oxidation. The test rods are filled to ~0.22 MPa (maximum 0.6 MPa) with tracer gases, e.g. Kr or He, to detect the onset of the rod failure with the mass spectrometer at the off-gas pipe.

Up to now, 17 bundle tests have been conducted; the main topics investigated are: hydrogen source term during reflood, influence of B_4C and Ag-In-Cd control rods on bundle degradation, effect of air ingress on oxidation and degradation of the core, and specific behaviour of VVER bundle geometry and materials during oxidation and reflood. One test was performed with the complete sequence including boil-off phase, pre-oxidation and

reflood. The QUENCH experiments will focus on the analysis of the relocation of cladding and fuel and the formation and cooling of in-core debris beds to gain information on the characteristics of the created debris particles. The main objective of these tests is the investigation of these processes under prototypical boundary conditions for a whole bundle.

As a result of the evaluation of the User Selection Panel the following experiment to be performed in the QUENCH facility was selected:

Title: QUENCH test with slow oxidation in air
Organisation: KFKI/AEKI, Budapest, Hungary

This test was successfully conducted on 27 July 2011 i.e. in month 18 of the project with a minor delay of 2 months as compared to the original planning.

Background
The high temperature interaction of fuel materials with air results in intense oxidation and nitriding of zirconium components. The oxidation heat can lead to temperature excursion and to the acceleration of bundle degradation. In case of severe reactor accidents air may have access to the core after lower head failure. Air oxidation can be expected in open reactor and spent fuel storage pool accidents as well. The safety significance of air ingress scenarios is emphasized by the formation of gaseous fission product oxides (e.g. ruthenium), which can dramatically increase the release of radioactive materials from the damaged fuel.
A number of previous out-of-pile bundle air ingress tests have been performed under a range of configurations and oxidizing conditions, namely CODEX AIT-1, AIT-2 with small 9-rod bundles, QUENCH-10 with 21-rod strong pre-oxidised bundle and PARAMETER-SF4 with finally melted 19-rod bundle. The accumulated data have demonstrated that air oxidation of cladding is a quite complicated phenomenon governed by numerous processes whose role can depend on the oxidizing conditions, the oxidation history and the details of the cladding material specification. The models for air oxidation do not yet cover the whole range of representative conditions. The main aims of new bundle tests should be the investigation of areas where data were mostly missing.

The QUENCH-16 bundle test with air ingress focussed on the following phenomena:
- Slow oxidation and nitriding of zirconium in high temperature air,
- Formation of oxide and nitride layers on the surface of Zr under oxygen starvation conditions,
- Breakaway oxidation of Zr in air, formation of spalling oxide scale,
- Reflooding of oxidised and nitrided bundle by water, release of nitrogen and hydrogen.

Pre-test calculations
The determination of the test protocol aimed at achieving the objectives was based on planning calculations by PSI (SCDAP/RELAP5), GRS (ATHLET-CD) and EDF (MAAP-4). A summary of these calculations is given in Table 1. The objective was to define the duration and the boundary conditions (power input, gas flow rates etc.) for different test phases (first column of the Table 1). Moreover, in addition, the code to code comparison was performed. In addition to the definition of the electric power vs. time curve, the main outcome was that the intended oxygen starvation period could be reached only with low air flow rates of approx. 0.2 g/s. None of the applied codes predicted temperature escalation during the reflood phase.

Table 1: Summary of results of pre-test calculations for the QUENCH-16 experiment.

Phase of experiment	Codes used to determine the test protocol		
	PSI (SCDAPSIM with PSI air))	GRS (ATHLET-CD)	EDF (MAAP)
Heat-up +Pre-oxidation	0-5000 s 10 kW 3 g/s steam 3 g/s Ar	0-2000-5000 s 3.85 → 10 kW 3 g/s steam 3 g/s Ar	0-5000 s 10 kW 3 g/s steam 3 g/s Ar
Cooldown	5000-6000 s 4.0 kW 3 g/s steam 3 g/s Ar	5000-6000 s 4.0 kW 3 g/s steam 3 g/s Ar	5000-6000 s 4.0 kW 3 g/s steam 3 g/s Ar
Air ingress	6000-ca.11700 (9260) s 4.0 kW 3 (1) g/s Ar 0.2 g/s air	6000-13500 s 4.0 kW 3 (1) g/s Ar 0.2 g/s air	6000-9000 s 4.0 kW 3 g/s Ar 0.2 g/s air
Quenching	11700 (9260) s (at 1823 K) 0/4 kW Fast injection, then 50 g/s water	12470 (9420) s (at 1823 K) 0 kW Fast injection, then 50 g/s water	9000 s (at 1823 K) 0 kW Fast injection, then 50 g/s water
Max. oxide after pre-oxidation	186 µm	190 µm	ca. 242 µm
Air ingress duration	5700 (3260) s	6470 (3420) s	3000 s
Oxygen starvation duration	3270 (1540) s	470 (920) s	1100 s
Remarks	- shorter air phase and almost no starvation for 0.5 g/s air - no influence of 0/4 kW during quench	- rapid temp. increase for 0.5 g/s air to >2000 K - activation of ZrN model causes higher temperatures and longer starvation time	- no variation of gas flow rates

Test conduct and results of on-line measurements

In common with the previous QUENCH experiments, the bundle was heated by a series of stepwise increases of electrical power from room temperature to a maximum of ~600 °C in an atmosphere of flowing argon (3 g/s) and superheated steam (3.3 g/s). The bundle was stabilised at this temperature, the electrical power being ~4 kW. During this time the operation of the various systems was checked.

In a first transient, the bundle was heated by power increase to about 1200 °C, reached at ca. 4000 s. This marked the start of the pre-oxidation phase to achieve a maximum cladding oxidation of up to 200 µm. The power was controlled via small increments from 10 kW to 11.5 kW, to maintain more or less constant temperatures. In line with pre-test planning calculations about 14 g of hydrogen were produced in this phase which lasted until 6300 s. At this point the power was reduced to 4 kW which effected a cooling of the bundle to 790 °C, as a preparation for the air ingress phase. This phase lasted 1000 s, until 7300 s. Towards the end of this phase, one of the corner rods was extracted from the test bundle for determination of the oxide thickness axial distribution. Preliminary measurement showed a maximum oxide thickness of 133 µm in the bundle what was within the target band.

In the subsequent air ingress phase, the steam flow was replaced by 0.2 g/s of air, and the argon flow was reduced to 1 g/s. The power was maintained at 4 kW. The change in flow conditions had the immediate effect of reducing the heat transfer so that the temperatures began to rise again. After some time measurements demonstrated gradually an increasing consumption of oxygen, accompanied by acceleration of the temperature increase at certain locations starting at about 10200 s. The faster increase was most marked at the mid elevations of the bundle. Oxygen was completely consumed at 10500 s. Shortly before that

time, partial consumption of the nitrogen was first observed, indicating local oxygen starvation which promoted the onset of nitriding. Following this, the temperature continued to increase until water injection was initiated at 11335 s when the maximum observed temperature was ca. 1600 °C at the 650 mm elevation. Thus there was a period of 835 s complete oxygen consumption and hence starvation in at least part of the bundle. The total uptakes of oxygen and nitrogen were about 58 and 29 g, respectively. The generally limited rate of temperature increase was the result of a rather low air flow rate, probably not untypical of reactor or spent fuel pond conditions.

Towards the end of the air ingress phase a second corner rod was removed. Some local spalling of the oxide scale was observed at elevation 300-900 mm. The white scales were spalled in the region between 350 and 650 mm, the lower sublayer has a yellow-brown colour typical for zirconium nitride.

Then reflood was initiated at 11335 s by simultaneously turning off the air flow, switching the argon injection to the top of the bundle, first rapidly filling the lower plenum of the test section with 4 kg of water, and continuing by injecting 53 g/s of water. The power remained at 4 kW during the reflood. Almost immediately after the start of reflood there was a temperature excursion in the mid to upper regions of the bundle (500 to 1400 mm), leading to maximum measured temperatures of about 2150 °C. Due to excess of the melting point of Zr, some bundle degradation is to be expected at these temperatures. Cooling was established at the hottest location ca. 70 s after the start of injection, but was delayed further at other locations. Reflood progressed rather slowly, perhaps due to the high temperatures and partial degradation, and final quench was achieved after about 500 s. In line with the temperature escalations, a significant quantity of hydrogen (128 g) was generated during the reflood. There are also indications of nitrogen release during the quench phase: 24 g from 29 g consumed during oxygen starvation period were released again due to the oxidation of nitrides. The recorded data are being processed for further analyses by participants within the LACOMECO and SARNET programmes.

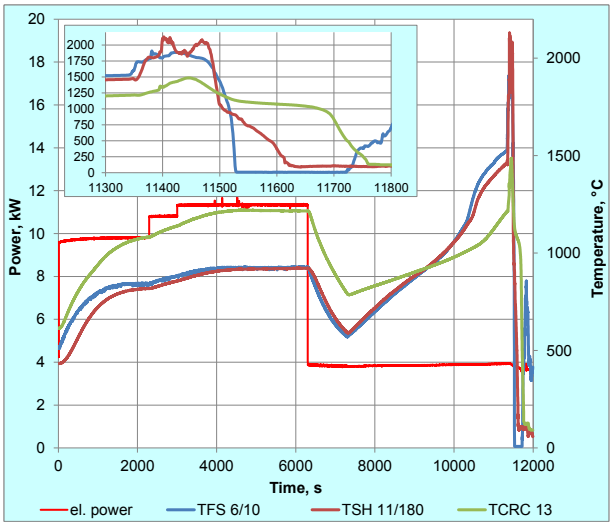

Fig. 1: QUENCH-16 test conduct showing electric power input and selected temperatures.

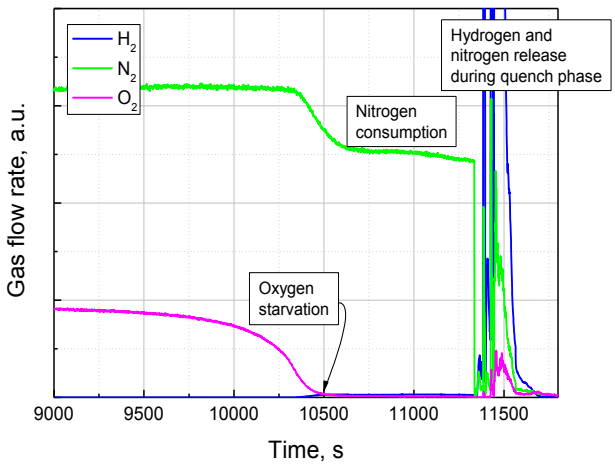

Fig. 2: Offgas analysis showing consumption of oxygen and nitrogen during air ingress phase and release of hydrogen and nitrogen during quench phase.

The shroud experienced similar temperatures to the bundle. As would be expected at such temperatures, the shroud failed ca. 40 s after initiation of reflood. Detection of Kr by the mass spectrometer indicated a first small failure of a fuel rod simulator soon after the start of oxygen starvation during the air ingress phase, and quite possibly further failures also during this phase. The videoscope inspection at the position of withdrawn corner rod B shows an intensive degradation of the oxide layer with partial spalling at bundle elevations between 450 and 750 mm. The frozen melt droplets and rivulets with oxidized surface were indicated between rods at lower elevations between –60 and 420 mm.

Post-test investigations

Metallographic investigations of corner rod D, withdrawn before reflood initiation, showed formation of porous nitrides inside the oxide layer as well as on the interface between oxide layer and α-Zr(O)-layer. The nitrides were formed at elevations above 350 mm under local or full oxygen starvation conditions. The investigation of the corner rod A withdrawn from the bundle after the test showed that nitrides were re-oxidized during the reflood with the formation of porous outer oxide sublayer at elevations 300 – 800 mm and growth of thick secondary inner oxide sublayer, formed due to steam penetration through the outer porous structure.

Fig. 3: Bundle cross section at 430 mm: frozen melt relocated from upper elevations.

Fig. 4: Bundle cross section at 830 mm: minor melting of some cladding segments.

After videoscope investigations the bundle (together with shroud and heat insulation) was extracted from the facility, disburdened from heat insulation and filled with the epoxy resin, which was hardened during two weeks. Then the bundle was cut at different elevations and corresponding cross sections were ground and polished. Metallographic investigation of cross sections showed formation of pools of partially oxidized frozen melt between 300 and 500 mm (Fig. 3) relocated from upper elevations 500 – 800 mm (Fig. 4).

A very intensive nitride formation was observed at elevations 350 – 500 mm (Fig. 5). The external oxide scales above residual nitrides have a porous structure due to re-oxidation of nitrides during reflood. At elevations above 550 mm only some nitride traces at the boundary between the inner dense and the partially spalled outer porous oxide scales were observed (Fig. 6). On the basis of measured nitrogen release during the quench phase

(24 g) and according to formula, the mass of hydrogen released during nitride re-oxidation was about 7 g.

The image analysis of frozen melt structures allows defining the degree of oxidation of the melt on the basis of the correlation between relative area of ceramic precipitations and content of oxygen transported into the melt. The measurement of melt areas at different elevations allows estimating the total hydrogen production by melt oxidation to be about 25 g.

A significant part of the hydrogen release during the quench phase can be interpreted as caused by intensive oxidation of the rod cladding and shroud metal (with formation of dense oxide sub-layer as shown in Fig. 6) by steam penetrated through the outer porous scale formed during the air ingress phase. The upper limit of the corresponding hydrogen amount can be estimated to 128 – 7 - 25 = 96 g.

The results of the experiment were presented at the 17th and 18th International QUENCH Workshops in November 2011 and 2012 correspondingly, as well as at the International Conference ICAPP'12 in June 2012, International Conference on Safety in Reactor Operations TopSafe 2012 and published as Scientific Report KIT-SR 7634 (Karlsruhe, 2013). Joint paper on the results of the pre-test calculations was presented at the ERMSAR-2012 Conference in March 2012. The test will be used for benchmark calculations in the WP5-COOL of SARNET2.

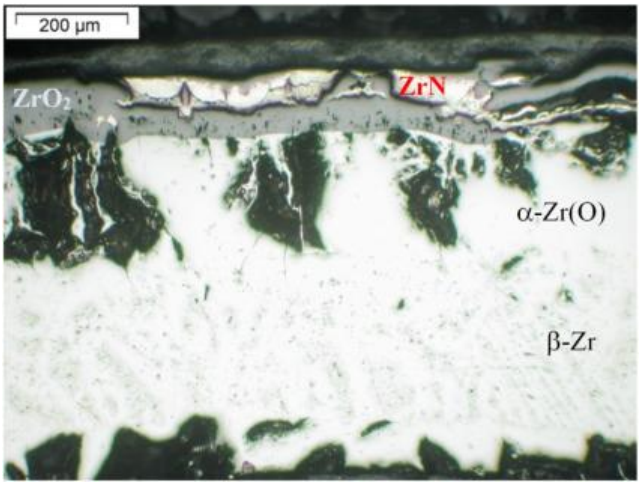

Fig. 5: Bundle elevation 350 mm: nitrides between two oxide layers.

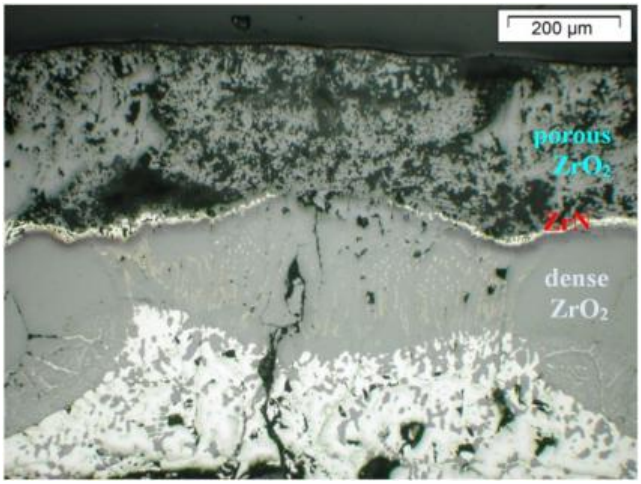

Fig. 6: Bundle elevation 550 mm: nitrides between inner dense and outer porous oxide layers.

3.3 WP2 LIVE

Cooling of core debris and behaviour of the stratified corium melt pool in the lower head are still critical issues in understanding of PWR core meltdown accidents. They were ranked as *high and medium priority issues by the SARP group of the SARNET NoE.*

A number of studies have already been performed to pursue the understanding of a severe accident with core melting, its course, major critical phases and timing and the influence of these processes on the accident progression. Uncertainties in modelling these phenomena and in the application to reactor scale will undoubtedly persist. These include e.g. formation

and growth of the in-core melt pool, relocation of molten material after the failure of the surrounding crust, characteristics of corium arrival in residual water in the lower head, corium stratifications in the lower head after the debris re-melting. These phenomena have a strong impact on a potential termination of a severe accident.

The main objective of the LIVE program at KIT is to study the late in-vessel core melt behaviour and core debris coolability both experimentally in large scale 3D geometry and in supporting separate-effects tests, and analytically using Computational Fluid Dynamics (CFD) codes in order to provide a reasonable estimate of the remaining uncertainty band under the aspect of safety assessment.

The main part of the LIVE test facility is a 1:5 scaled RPV of a typical pressurized water reactor. The inner diameter of the test vessel is 1 m and the wall thickness is 25 mm. The material of the test vessel is stainless steel. To simulate the decay heat, heaters are used, which provide in different layers a representative and homogeneous heating of the melt in the lower head. The core melt is simulated by different materials. These materials should, to the greatest extent possible, represent the real core materials in important physical properties and in thermo-dynamic and thermo-hydraulic behaviour. Important criteria are that the simulant melt should be a non-eutectic mixture of several components with a distinctive solidus-liquidus area of about 100 K, and that the simulant melts should have a similar solidification and crust formation behaviour as the oxidic corium. To investigate special problems a mixture of nitrates is used with a melting temperature of about 350 °C, and with a phase diagram similar to the expected core melt.

For different melt masses in the lower head the heat flux through the vessel wall can be determined by thermocouples at the inner (IT) and outer (OT) vessel wall, which provide a 3D picture of hot zones in the wall and possible failure modes of the lower head.

Due to the ability to flood the melt in-vessel, particle bed formation and/or gap cooling with a resulting stop of the anticipated accident can be investigated at different stages of the accident scenario.

The information obtained from the LIVE experiments includes heat flux distribution along the reactor pressure vessel wall in transient and steady state conditions, crust growth velocity and influence of the crust formation on the heat flux distribution along the vessel wall. Supporting post-test analysis contributes to characterization of solidification processes of binary non-eutectic melts. Complementary to other international programs with real corium melts (like METCOR-P, PRECOS, and INVECOR projects of the International Science and Technology Center (ISTC)), the results of the LIVE experiments provide data for a better understanding of in-core corium pool behaviour. The results of the LIVE experiments allow a direct comparison with findings obtained earlier in other experimental programs (SIMECO, ACOPO, BALI, etc.) and are being used for the development and assessment of mechanistic models for description of in-core molten pool behaviour and their implementation in the severe accident codes such as ASTEC. Moreover, the obtaining of 3D data has become more important, as it is now clear that the direct extrapolation of the results of 2D experiments may be inappropriate.

As a result of the evaluation of the User Selection Panel the following experiment to be performed in the LIVE facility was selected:

Title: Dissolution kinetics of a pure KNO_3 crust by a $KNO_3/NaNO_3$ melt (LIVE-CERAM)
Organisation: CEA, Grenoble, France

The experiment aims at examination the dissolution kinetics of a pure KNO_3 crust by a $KNO_3/NaNO_3$ mixture. There exist only scarce data on corium/refractory material interaction. Former experiments addressed mainly the final steady state situation or used smaller scales. No detailed data are available for transient corium/refractory material interaction in 3D geometry. The test will be performed using simulant materials (KNO_3 as refractory material (melting temperature ~340°C) and a KNO_3-$NaNO_3$ melt at the azeotropic composition (melting temperature ~222°C). This will be an excellent simulation of the refractory core-catcher ablation by a lower temperature multi-component melt in a severe accident. It would address two SARP issues: corium coolability in lower head and ex-vessel melt pool configuration during MCCI. Pre-test and post-test analysis will be done by CEA (various models). This is a good example for the use of an in-vessel facility for an ex-vessel research and so increasing the value and application of the facility. The project will require 2 tests with a precursory test to produce the refractory layer and this will give additional data on single component melt behaviour in comparison with multi-component melts.

The LIVE-Ceram test programme included several trials for the formation of the KNO_3 liner and two ablation tests. Due to the complexity of the experiment, substantial modifications of the test facility and the heating system were necessary. The LIVE-CERAM test programme started then with several pre-tests to check the feasibility of crust generation method and with pre-test calculations. These pre-tests have been performed in October 2011, i.e. in month 21 of the project with 9 months delay as compared to the original planning. The final test for the formation of the KNO_3 liner was performed in December 2011. The Ablation test I was successfully conducted on the 24th-25th January 2012 and the ablation test II on the 1st March 2012.

Background
There is large interest of the international scientific community for core-catcher design methodologies considering not only steady state situations but also transient behaviour. However, only scarce data exist on corium-refractory material interaction for the design of refractory liners for core catchers and for protection of concrete walls which should be applied in LWRs and LMFBRs. The experiments at CIT (Saint Petersburg) addressed mainly the final steady state situation. Simultaneous Corium-Concrete-Zirconia Interaction experiment has been performed by Areva (Erlangen) in small scale. No detailed transient data are available for corium-refractory material interaction for 2D geometry.

Based on this background LIVE-CERAM experiment will provide data of transient 2D corium-refractory material interaction. The experiment should simulate the ablation process of a high-melting temperature refractory material by low-melting temperature corium. Due to the dissolution of the refractory material into the boundary area and in the bulk corium, the boundary layer and the bulk melt are expected to be gradually enriched in the refractory material, which leads to an increase of bulk melt melting temperature and boundary temperature.

In the LIVE-CERAM experiment, the initial pure KNO_3 (melting temperature of ~340°C) simulates the refractory material, and the eutectic mixture of 50 mole% KNO_3 - 50 mole% $NaNO_3$ (melting temperature of ~222°C) simulates the corium. A ~8 cm crust of pure KNO_3 should be firstly generated along the semi-spherical vessel wall; afterwards the eutectic

melt is poured in the vessel. During the ablation process, the liquid melt is homogenous heated and its temperature should not exceed the melting temperature of the pure KNO_3. The evolution of melt temperature and interface temperature are measured at several latitudes.

Definition of the experimental performance:
For the decision of experimental method and the definition of the test parameters, CEA Grenoble and KIT held a partners meeting at KIT on May 26 2011. The whole test comprises 2 separate operations: crust formation and ablation test. The test conditions have been defined as following:

Generation of KNO_3 crust:

- The heating basket and all the heating elements should be repositioned 63 mm higher, so that the gap between the heating elements and the vessel wall is 8 cm (Fig. 7). Heating elements remain in the vessel during the creation of the crust.
- A low heating power should be only dissipated in the lower part of the pool to enable a formation of relatively uniform crust layer
- The height of KNO_3 crust is 435 mm and the height of the eutectic melt pool is 385 mm to avoid the overflow of the liquid melt into the gap between the vessel and the KNO_3 layer.
- Four thermocouple trees are mounted at polar angles 0°, 37°, 52° and 66°. The distance between neighbour thermocouples is 0.5 cm at polar angle 52° and 66°, and 1 cm at polar angle 0° and 37°. The length of the trees will be ~10 cm (2 cm longer than the layer thickness of the KNO_3 crust).
- The vessel is externally cooled by water with flow rate of 1.3 kg/s.

Ablation test:

- The melt pouring temperature is about 260°C. The maximum melt pool temperature is 330°C, which is slightly lower than the melting temperature of KNO_3 (334°C). The maximum heating element surface temperature is allowed to be slightly higher than the maximum bulk melt temperature.
- The melt is heated with 7 kW homogenously at the beginning. If the melt temperature reaches 330°C after some time, the heating power will be reduced. After the decrease of melt temperature the heating power will be increased to 7 kW again and will be kept at this level until the steady state will be reached.
- The criterion for the end of the test is the approach of steady melt temperature and the steady crust temperature at polar angles 52° and 66°.
- Melt samples are taken every 15 minutes at beginning and then every 30 minutes. Residue crust will be analysed after the test.
- Two measuring positions with the crust detection lance are foreseen.

Test performance and results
For the generation of a uniform KNO_3 crust layer two trials have been conducted on the 5th and the 7th December 2011 respectively. The first trial was named crust formation test. The height of the crust was 435 mm. Since a large gap (~ 1 cm width) was formed between the crust and the vessel wall after the crust formation test, a second trial of melt pouring was conducted to fill the gap. The crust height after the gap filling test was 450 mm. The crust thickness runs smoothly from ~4 cm to 12 cm from upper range to the lower region. Fig. 8 shows the crust profile after the gap filling test.

During the Ablation test 1, 177.5 kg eutectic melt, corresponding 93.4 liter, was poured into the vessel. The initial temperature of the melt pool was 265 °C. External water cooling with 1.3 kg/s flow rate was started before the melt pouring. A total heating power generation of 7 kW was dissipated volumetrically in the liquid pool for the initial pool geometry. At the end of the test 218 kg melt was extracted back to the heating furnace. Thus 40.5 kg KNO_3 crust, corresponding to 21.7 liter, was ablated at the end of the Ablation 1 test. The final KNO_3 concentration in the liquid melt was 60.3 mole%.

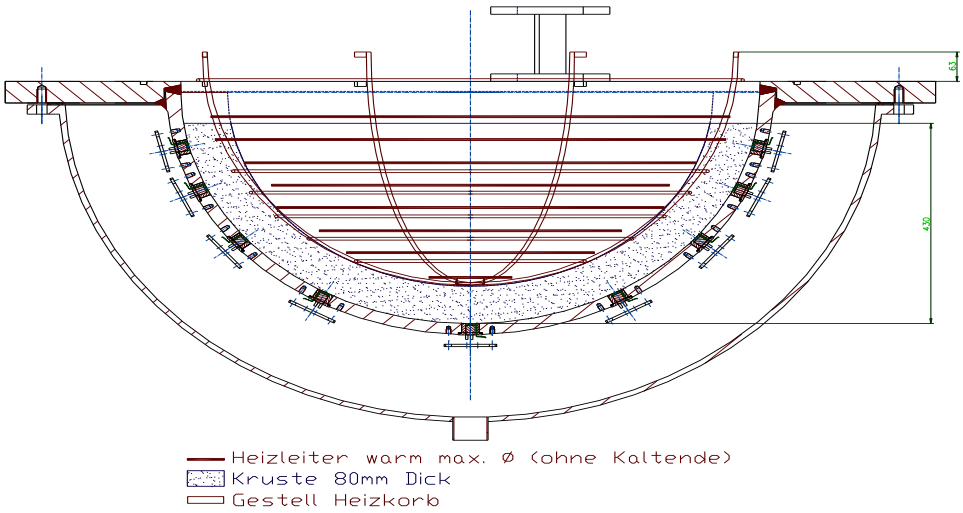

Fig. 7: Position of the heating basket for the generation of 8 cm thick crust layer.

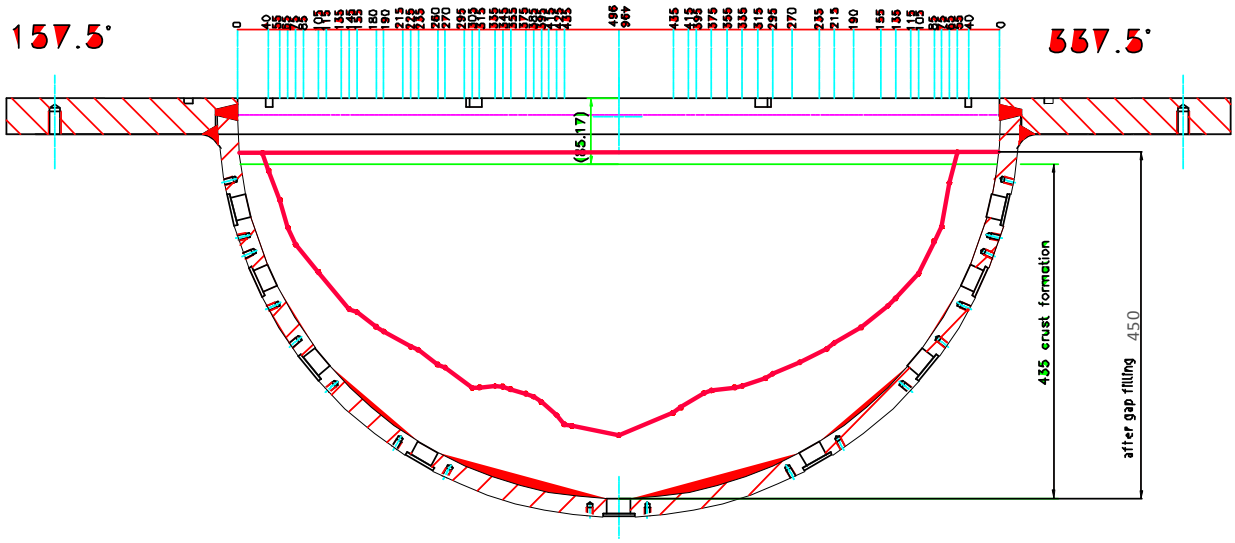

Fig. 8: KNO_3 crust thickness profiles after gap filling test.

210 kg melt was poured in the test vessel during the Ablation test 2. The pouring temperature of the melt was 274 °C. The melt pool height was 375 mm, which was 10 mm lower than the upper edge of the crust. The original melt liquidus temperature was 232.5 °C, corresponding to a composition of 58.4% KNO_3 - 41.6 % $NaNO_3$. At the end of the test 234 kg of melt was extracted out of the vessel. Therefore 24 kg of crust was ablated during

the Ablation 2 test. The melt liquidus temperature before melt extraction was 240.7 °C, corresponding to 62.1 mole% KNO_3 in the melt.
Totally 15 kW heating power was volumetrically released from 5 planes of heating element in liquid pool.

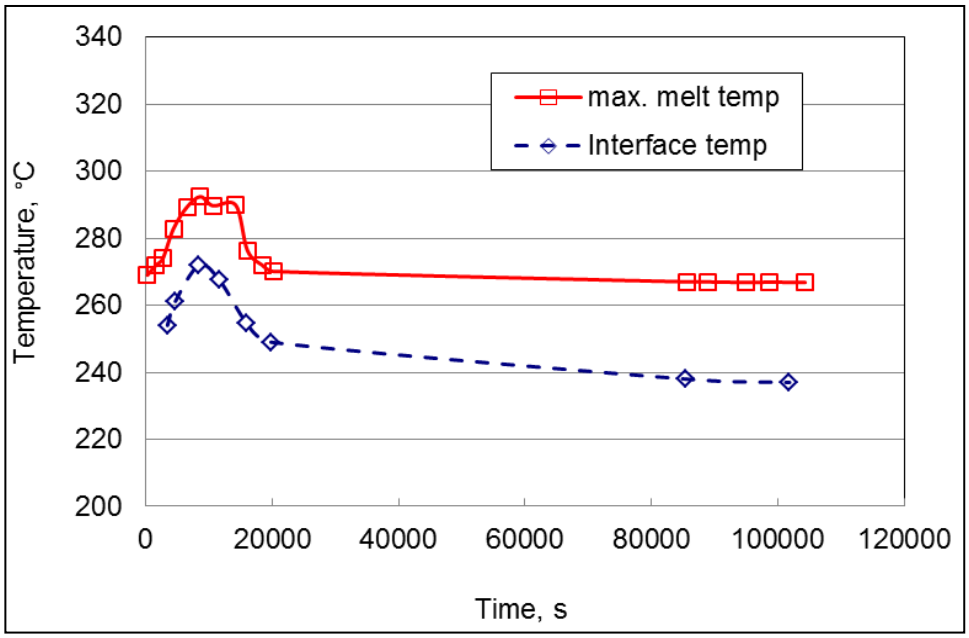

Fig. 9: Maximum melt temperature and melt/crust boundary temperature during the ablation 1 test.

Fig. 9 shows the maximum melt and interface temperatures. An important observation is that the melt temperature did not exceed 295°C (well below 336°C corresponding to the melting temperature of KNO_3) during the whole test and that the refractory material was dissolved into the melt. The maximum melt temperature was located in the top region of the melt, as was the case in the natural-convection test without dissolution. The maximum (~292 °C) was reached after approximately 10 000 seconds. Beyond 10 000 sec, the melt temperature decreased significantly during another period lasting 10 000 seconds (270 °C temperature reached after 20 000 sec), tending towards the final steady state temperature (267 °C) after approximately 1 day. It can be observed that the maximum melt temperature in fact followed the evolution of the measured interface temperature, with a difference of about 20°C to 30 °C. The interface temperature increased to about 270°C after ~10 000 sec and then dropped to 249°C at 20 000 seconds. The interface temperature was 237°C at the end of the test.

The evolution of the KNO_3 concentration in the melt is shown in Fig. 10. The melt composition stayed initially constant at the eutectic (pouring) concentration until ~5000 seconds. The melt temperature at that time had increased to 280°C and the interface temperature to ~260°C. After t~5000 seconds the KNO_3 concentration in the melt increased significantly and reached ~58 mole % after ~20 000 seconds. At that time, the melt and interface temperature had significantly decreased. At the end, the KNO_3 mass concentration in the melt was about 60 mole %, which corresponds to a liquidus temperature of ~237°C, equal to the interface temperature measured at the end. The melt sample taken from the bottom has the same composition as the melt sample taken at the top. This indicates homogenization of the melt composition by internal convection.

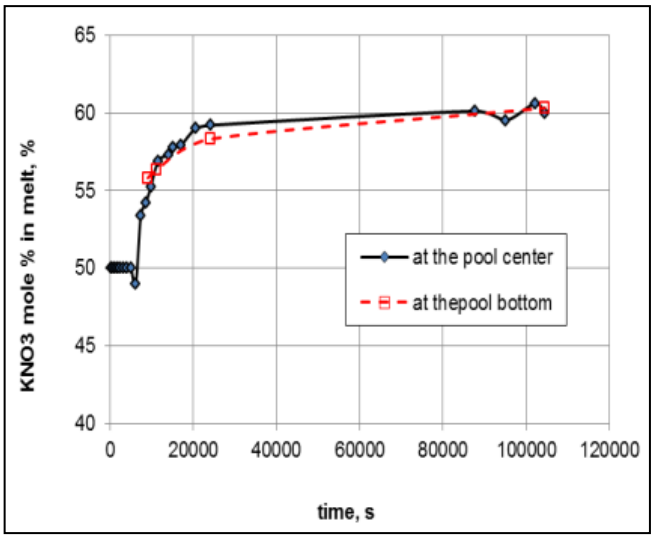

Fig. 10: Evolution of the bulk melt composition.

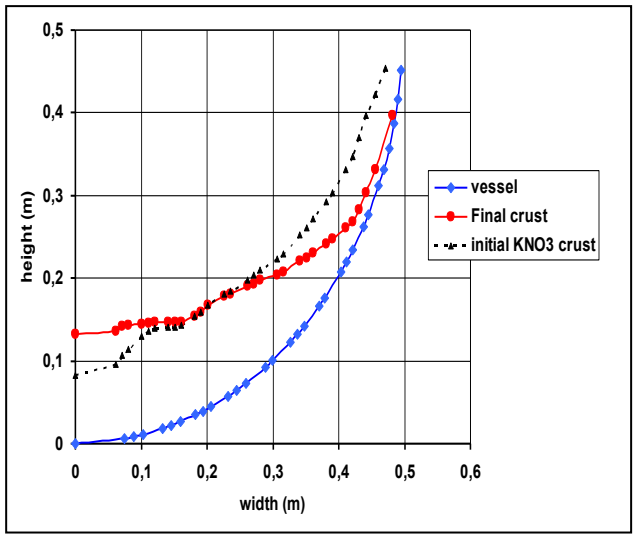

Fig. 11: Shape of crust thickness distribution.

The shape of the crust before and after the Ablation test 1 is shown in Fig. 11. The upper part of the crust was significantly dissolved (polar angle > 30°). It is also apparent that some solid was deposited at the cavity bottom. Analysis of the composition of the crust showed that the residual crust material was mainly KNO_3.

Analytical Interpretation by CEA

A simple 0D model has been developed for the purpose of phenomenological analysis. By coupling the heat transfer and mass transfer, the interface temperature, the progression of the interface temperature, pool liquidus temperature and the maximum pool temperature can be predicted, as shown in Fig. 12 for the reference case similar to the Ablation test 1.

During the dissolution transient, the interface temperature rises above the liquidus temperature corresponding to the actual average pool composition. Interpretation using the 0D model shows that this behaviour is linked to enrichment of the liquid with refractory species at the interface. The mass transfer kinetics between the interface and the bulk is controlled by a diffusion sublayer. The 0D model yields a reasonable fit with experimental results, even if there is room for further optimization of calculation of the mass transfer coefficient. The assumption that $T_{interface} = T_{liquidus}$ during the whole transient correctly predicts the ablation delay and final pool and interface temperatures, but underestimates the transient melt temperature.

A 1D model approach has been developed to describe non-uniform axial ablation of the crust. This model combines a 1D description of boundary-layer flow on a curved interface and a 1D description of the temperature distribution on the pool axis.

Boundary-layer flow is described by an integral boundary layer model involving mass, momentum and energy balances. To calculate the dissolution rate still holds locally. Heat transfer is calculated locally, as a function of the local temperature difference between the bulk and the interface and of the local heat transfer coefficient associated to the laminar boundary flow. In the 1D approach, the characteristic scale is the local thickness of the dynamic boundary layer. Thus Nu and Sh correlations are based on this local scale: The evolution of the calculated crust thickness is given in Fig. 13.

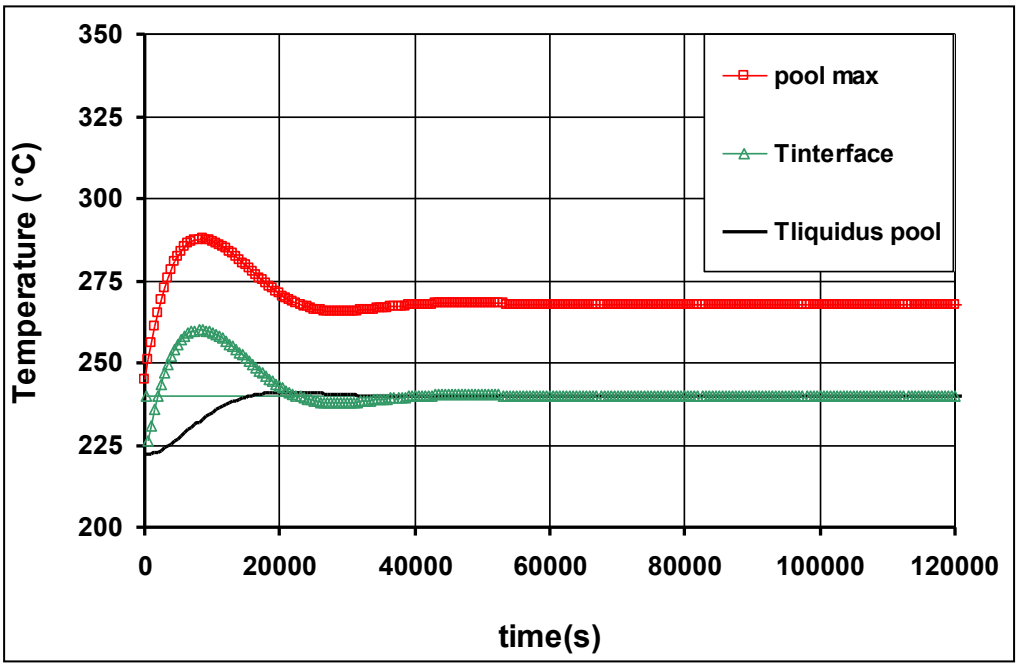

Fig. 12: Calculated temperature evolution in the reference case.

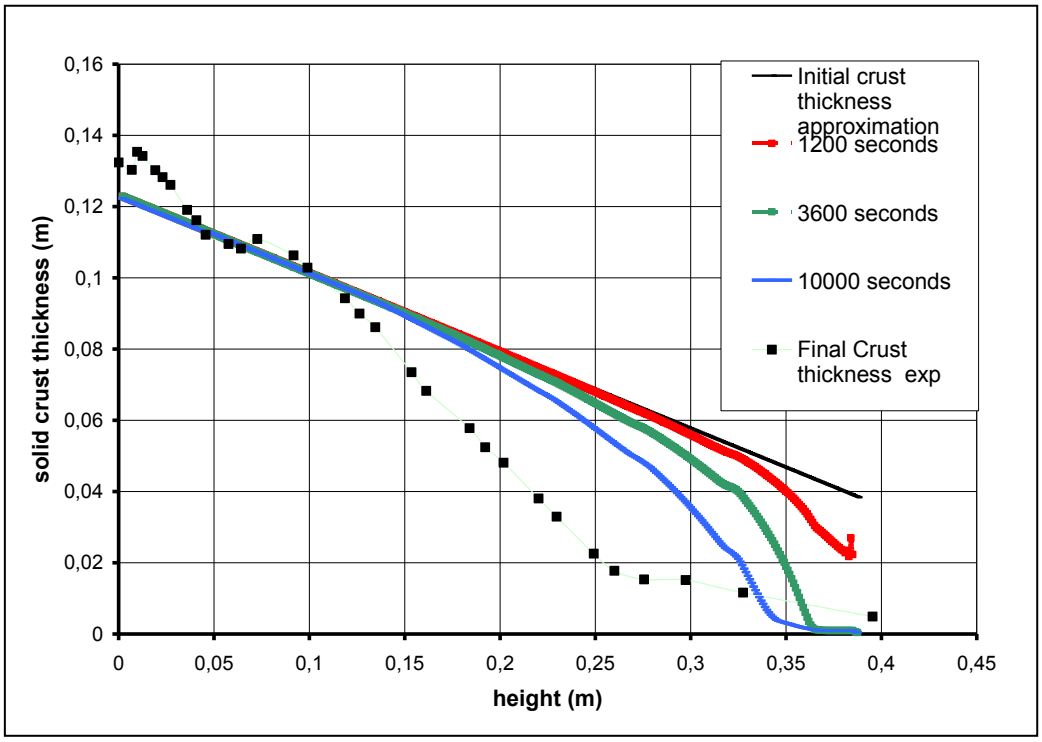

Fig. 13: Results from 1D model; evolution of crust thickness distribution.

Analysis with a 1D model approach indicates that the interface temperature is not uniformly distributed during the ablation transient. This behaviour is linked to non-uniform distribution of the ablation rate and heat flux. Although heat flux is non-uniform in the final steady state, the interface temperature becomes uniform, equal to the liquidus temperature of the bulk when the ablation rate tends towards zero.

In the case of the LIVE-CERAM experiment, density variations due to solutal effects could be neglected. This would in general not be the case with other materials. If the ablated

material has lower density than the melt, the consequence could be reverse convection in the melt during the ablation transient, in comparison with the natural thermal convection (because the density of the liquid in the boundary layer can be lower than that of the bulk liquid). This case deserves further investigation.

3.4 WP3 DISCO

The DCH issue was assessed as *medium priority by the SARP group of the SARNET NoE meaning that the programmes are to be continued as planned or at reduced effort.* The involved SARNET partners (KIT, IRSN, GRS, EDF and TUS) concluded that the uncertainty in the code calculations is still too large to assess the risk of containment failure for certain reactor geometries due to the lack of validated models, especially for the extrapolation to reactor scale.

Moreover, the available experimental data from DCH tests in the DISCO facility clearly demonstrated that the scaling of combustion of hydrogen jets in air-steam-hydrogen atmospheres must be established by applying combustion codes (e.g. COM3D, REACFLOW), and the resulting H_2 combustion data (enthalpy, etc.) must be transferred to the codes modelling DCH. Combustion and heat loss models still need further improvements. However, experiments at a single scale are not sufficient to achieve this. Therefore additional tests addressing the combustion of hydrogen jets in air-steam-hydrogen atmospheres at different scales are necessary. This issue is ranked as *high priority by the SARP group of the SARNET NoE* and is clearly linked to the WP4 HYKA, where these topics will be addressed.

The consequences of DCH are essentially related to the reactor cavity geometry. Therefore an experimental database has been established for the plant types EPR, French PWRs and some of VVERs. For other plant specific geometries the experiments must still be conducted. The recent studies indicated that the need to investigate DCH in boiling water reactors (BWR) may arise. Moreover, other still unresolved issues are the influence of water in the reactor cavity and fission products release during DCH and its impact on the overall source term, which has not sufficiently been investigated before. The DISCO experimental facility is the only one available worldwide, that can address these critical issues.

The DISCO facility is designed to perform scaled experiments that simulate melt ejection from the RPV to the reactor cavity after the RPV failure under low system pressure during severe accidents in LWRs. These experiments are devised to investigate the fluid-dynamic, thermal and chemical processes during melt ejection out of a breach in the lower head of an LWR pressure vessel at pressures below 2 MPa with an iron-alumina thermite melt (~2000 °C) and steam. The position, size and shape of the failure can be varied. The containment is modelled by a pressure vessel with a volume of 14 m³, rated at 1 MPa. The combined volumes of the reactor pressure vessel and reactor cooling system are modelled by a vessel with a volume of 0.08 m³, rated at 2 MPa and 220 °C. The geometry of the reactor pit and reactor sub-compartments is adapted according to the investigated reactor type. The atmosphere in the containment is variable (inert, air, steam or a mixture, including hydrogen).

As a result of the evaluation of the User Selection Panel the following experiment to be performed in the DISCO facility was selected:

Title: Ex-vessel fuel coolant interaction experiment in the DISCO facility
Organisation: IRSN, Fontenay aux Roses, France

This experiment, called DISCO-FCI, is related to a DCH test using a pit full of water and so represented a FCI test as much as a DCH and is of great interest to reactor safety. The main phenomena are the use of the Fe-Al_2O_3 thermite melt in a steam/air/H_2 atmosphere and the injection of the melt under pressure into the flooded pit. This pressured melt injection into the water is also an aspect that is relatively little researched. This is linked to fuel coolant interaction (WP7.1) and to debris formation (WP5.3) as well as MCCI (WP6.3) and H_2 behaviour in containment (WP7.2) of SARNET2. This will also be linked to the ongoing OECD SERENA-II project. Although there is a certain risk of steam explosion, the risk is considered as low because of the strength of the facility construction as well as the probability of its occurrence (no external triggering and limited mass of melt). Topics addressed in this test were ranked as high (FCI) and medium (DCH) priority issues by the SARP group of SARNET.
Due to the complexity of the experiment like substantial re-design and modifications of the cavity and RPV and necessity to perform additional pre-test analysis, the test was successfully performed on the 14th September 2011, i.e. in month 20 of the project with 8 months delay as compared to the original planning. The results were distributed to SARNET2 WP7-CONT partners for analysis and interpretation.

Short preliminary description
Fig. 14 shows a generic representation of the DISCO facility which is composed of several parts simulating the containment: the reactor cooling system (RCS), the RPV, the pit and sub-compartments. A scheme of RPV and dimensions of the cavity are given in Fig. 15.
In the present experiment, the arrangement is close to a French 900 MWe reactor but it does not reproduce precisely a given reactor. The pit zone was modified in order to have the largest water pool as possible. Compared to a 900 MWe reactor pit, the scale is approximately 1:10.
The fuel is a melt of iron-alumina with a temperature of about 2400 K, obtained from a thermite reaction initiated directly inside the vessel (RPV) some few seconds before its delivery to the pit through a nozzle. The delivery occurs thanks to the melting of a brass fuse inside the nozzle. Before the delivery, the vessel pressure can be adjusted thanks to a steam accumulator. The nozzle diameter was set to 0.03 m which corresponds roughly to 0.30 m at reactor scale.
The primary circuit is simplified and simulated with one single vessel. Inside this vessel, two zones represent the RPV and the RCS, linked with a system of small pipes to adjust pressure loss (found to have no real impact in fact).
The gas initial composition in the containment can be adjusted with air, vapor and hydrogen. In the present test, no hydrogen is initially present (to limit combustion) and the containment atmosphere is made with 1 bar of air and 1 bar of vapor. The level of the water in the pit is about 0.54 m, just below the nozzle outlet (the vessel was not submerged to limit problems related to brass fuse melting). It was heated to 85 °C in order to yield a subcooling in the range of expected ones in a reactor situation. The main characteristics of the test are given in Table 2.

Table 2: Main parameters of the test.

Pressure in RPV at melt delivery	1.02 MPa
Nozzle diameter	0.03 m
Melt mass	10,6 kg
Pressure in containment vessel	0.2 Mpa
Gas composition in containment vessel	50 % air, 50 % vapor (no H_2)
Water temperature	85 °C

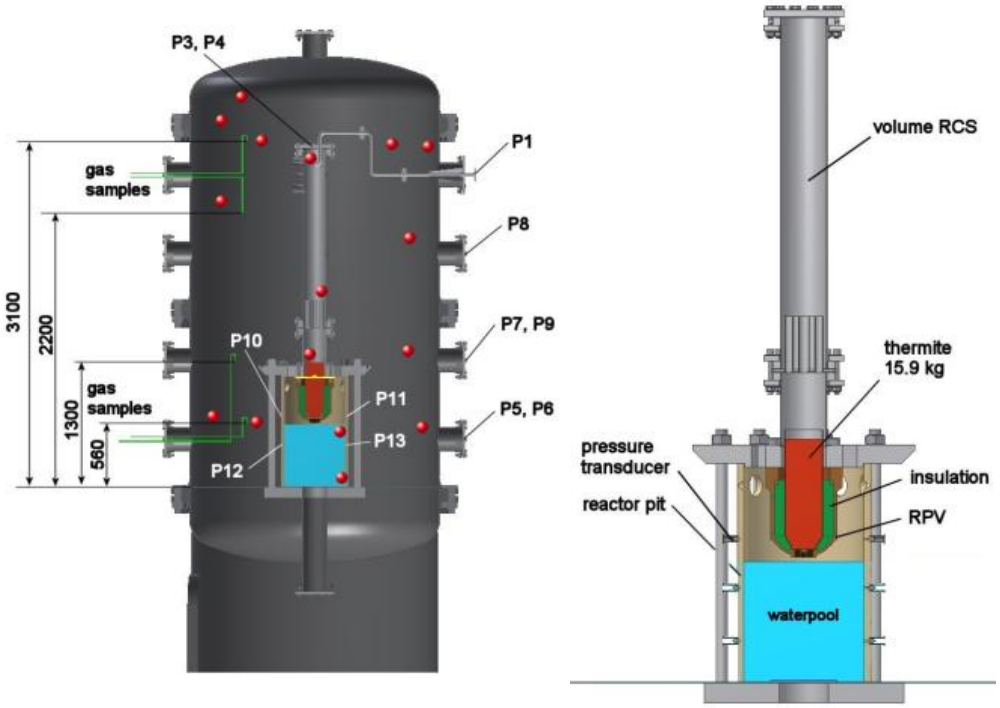

Fig. 14: Containment pressure vessel and internal structures of RPV/RCS vessel and cavity.

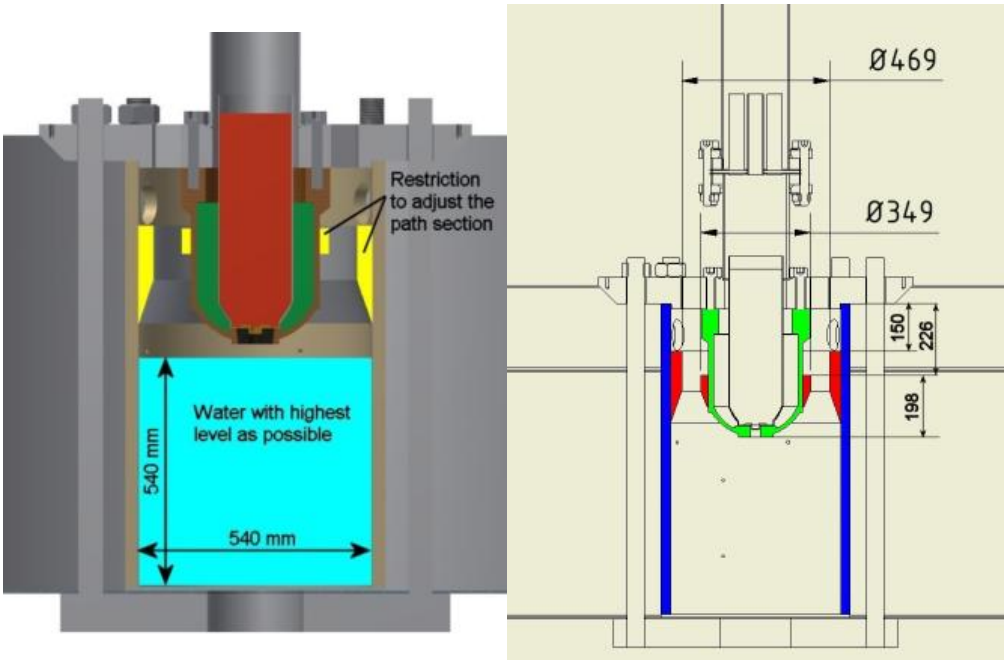

Fig. 15: Scheme of RPV and dimensions of the cavity.

Description of the test behaviour

The steam pressure of accumulator is initially at 0.92 MPa (Fig. 16). The initial pressure in the vessel is 0.1 MPa. After a first phase of melt burning, the pressure rises to about 0.4 MPa. When the valve of the accumulator is open, the pressure in the RPV rises to about 0.82 MPa. Fig. 17 shows the pressure in the cavity, containment and RPV over a shorter time. The exact initial pressure value in DISCO containment vessel is equal to 0.192 MPa. The final pressure reached in cavity and containment is equal to 0.24 MPa. The pressure increasing in the containment is about 0.04 MPa for the first second of the test, up to equilibration with the RCS RPV. It is noticed that a small decrease occurs followed by a slow increase which was not observed in the DCH tests. The pressure rise stops after about 15 seconds.

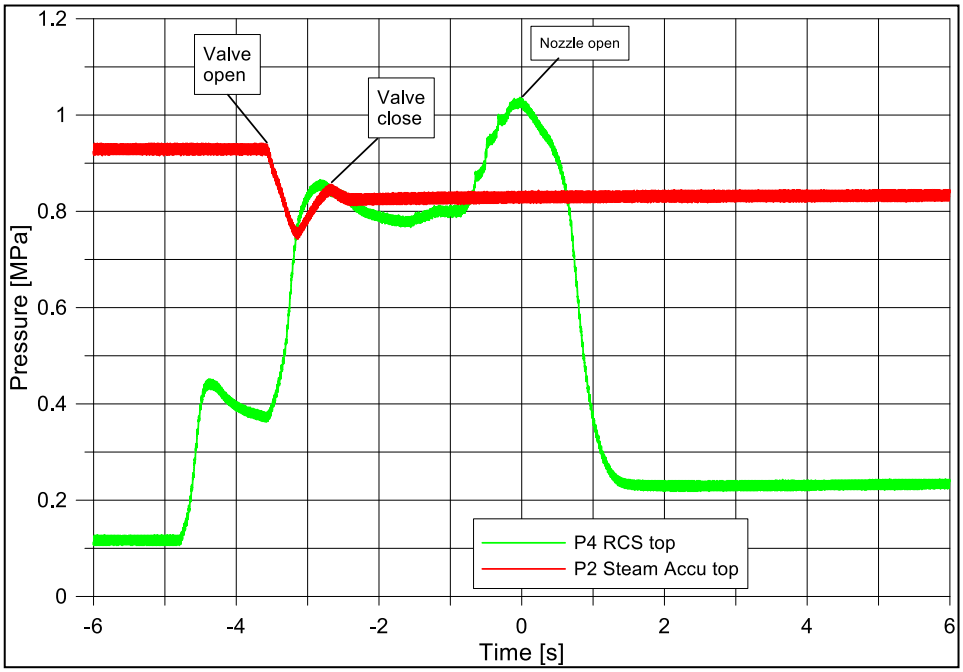

Fig. 16: Pressure in steam accumulator and RPV.

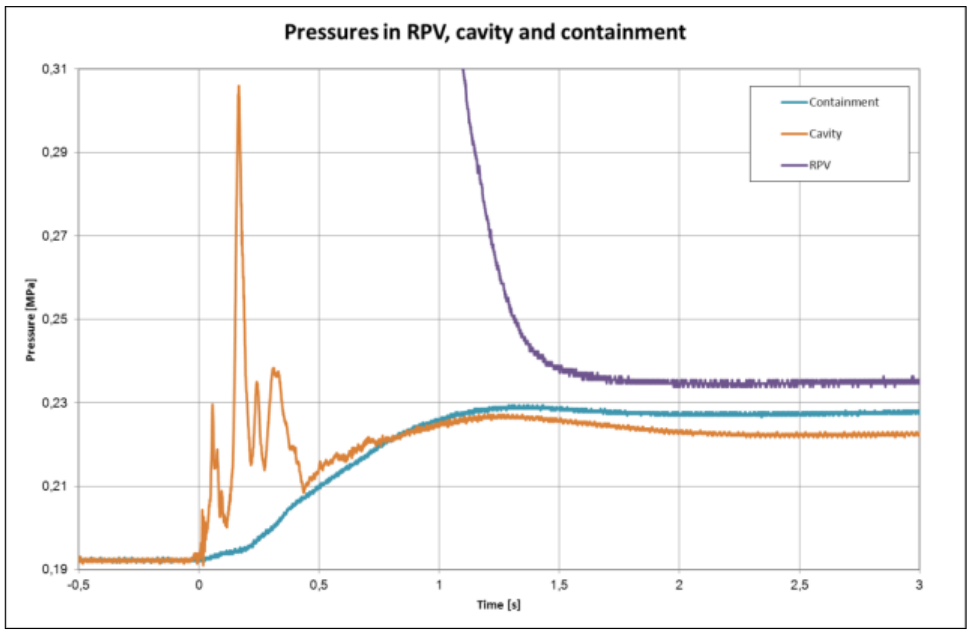

Fig. 17: Pressure in cavity (short time).

It is noted that the pressure then further rises in the last second and reach 1.02 MPa when the brass plug melts and delivers the fuel. Time 0 is chosen to correspond to the time of melt delivery. Regarding the cavity, we obtain a series of small peak of pressure during the first 0.5 second. The highest of this peak shows a pressurization of about 0.1 MPa at t=0.17 s. This peak cannot be attributed to a steam explosion. The pressure inside the cavity becomes homogeneous at the beginning of this peak. The pressure equilibration with the containment occurs a bit after 0.6 s.

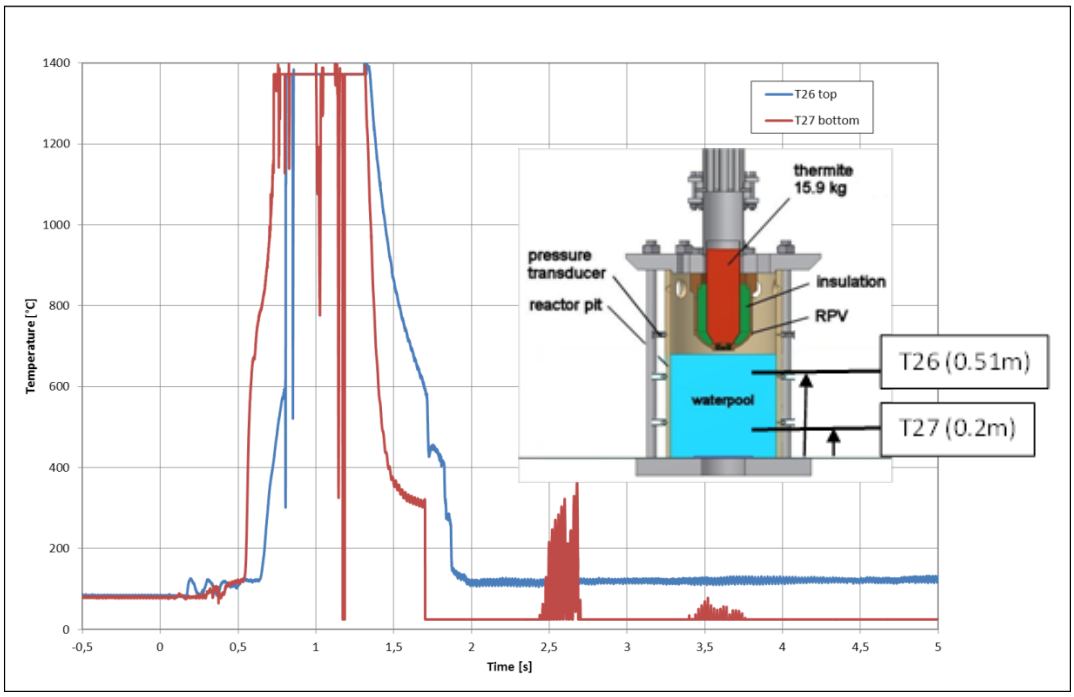

Fig. 18: Temperature in cavity.

An increase of temperature was observed which is slower than the pressure increase. This indicates that the second slow pressure rise after 1 s is due to a slow temperature increase that could be related either to heat up by debris (but it should be seen also in DCH tests), either to further boiling in the debris zone, either to slow combustion. This maximal value of temperature is essentially localized at the top part of the containment.
After 12 s, the temperature reaches a maximum value of 130°C (403 K) while the temperature in the lower part of the containment is at about 105°C (377 K). This might indicate that the temperature rise is due to slow combustion of hydrogen accumulated in the upper part of the vessel and propagating downward. The temperatures then slowly decrease due to heat losses and temperature slow equilibration in the various part of the vessel. The high temperature observed in the cavity (Fig. 18) after 0.5 s might indicate the disappearance of water (ejection) from the cavity.

Post-test analysis
The water inside the cavity has been almost totally ejected since only 5 kg out of the initial 125 kg remained in cavity. The ejection should be due for a part to the blow down of the gas initially present in the RPV/RCS.
About 66 % of the melt was found remained on the cavity floor as a compact crust. It is seen to be with high roughness, likely to come from the impact of fragmented drops. The crust thickness is not fully homogenous. The “hole” in the middle indicates that the jet impacted on the floor. The melt slipped along the wall only for few centimeters. The cavity

walls are then found quite clean. This is different from the DCH test (no water in cavity) where the remaining melt was on the form of smooth layers, indicating then a late solidification.
In the present case, it is then likely that partial solidification of the melt at impact on the floor play a role in the retention of the melt in the cavity. Similarly, only few melt stayed stuck to the external side of the RPV, compared to DCH tests. Again, it is found in the form of local accumulation of melt drops rapidly solidified close the nozzle and the rest of the RPV was almost protected. This would indicate that melt was transported out of the pit with the water. It is however expected from the analyses for DCH tests that gas blow-down (following the water ejection) alone would not lead to an important ejection considering the rather low vessel pressure. Approximately 7 % of the melt was found inside the RPV. The thick layer is nevertheless thought to be due to the melting process. 10 % of melt was found in the RCS part, likely to come from a melt ejection due to some interaction with the water. Approximately 10 % of the melt was transported to the subcompartment, with the water, where it formed a kind of mud that could be easily collected. It is likely then that the melt was transported by water and rapidly solidified. Part of the melt ejected inside the containment dome was found stuck on the upper part of this dome. It is in the form of very small particles. Water was also found on the upper dome surface. We can note that the balance imprecision is estimated to ~ 10 %.
Based on the results, we might estimate that the fragmentation grade was only about 30 % of the ejected melt and thus the jet impacted the bottom of the section essentially in a compact form. Very roughly, this might indicate a breakup length (length to break totally the jet in the absence of floor) of 3 times the water height, i.e. about 15 cm, i.e. a dimensionless length L/D of roughly 50, a consistent but quite high value compared to usual data (about 20). However, it is also possible that the largest particles impacted the floor while still molten and formed a compact crust.
The fragmented debris was sieved. The mass partition depends on the sieving itself and it is better to show it as a probability density distribution, shown in Fig. 19 for the total debris mass. The size distribution (mass) indicates tendency to small particles (unlike mass sieving partition). The distribution is only roughly log-normal (curve shown: with same median and mean mass size). The analyses concerning the different averaged diameters are the following:

- Mean Sauter[1] = 160 µm
- Median size = 0,4 mm
- Mean mass size = 0,7 mm

The size of the particles is very small compared to classical data, despite a smaller melt density compared to corium. This might be due for a part to the high expected velocity of the jet. A rough estimate of the ejection velocity is obtained with

$V_j \approx \sqrt{\frac{DP}{\rho_j}}$ which indicates a velocity of about 14 m/s.

Nevertheless, the size is small and it is possible, as already said, that some larger particles were still molten when impacting floors and walls. In such case, the debris size is representative only on the solidified debris before they reach a wall.

[1] Sauter mean diameter (SMD, d32 or D[3, 2]) is an average of particle size. It is defined as the diameter of a sphere that has the same volume/surface area ratio as a particle of interest.

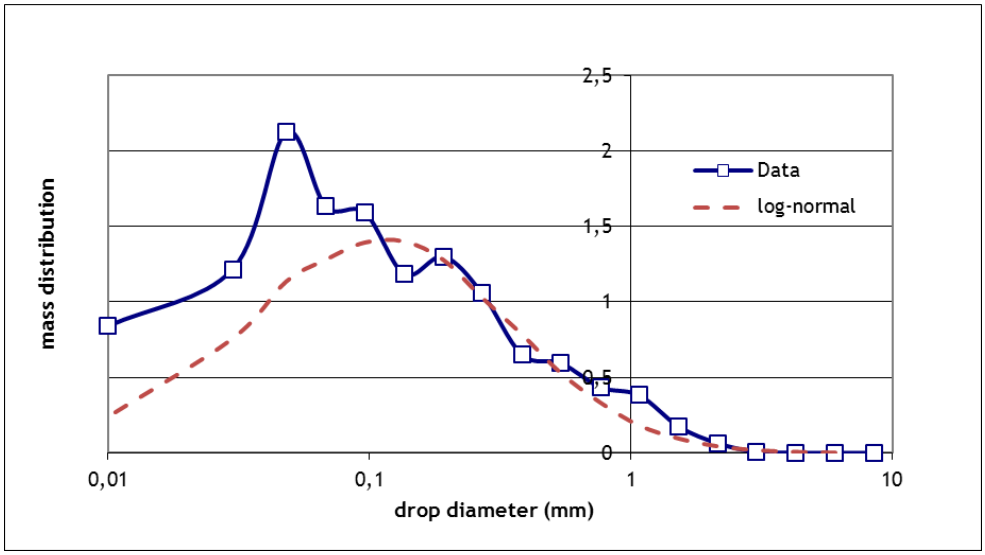

Fig. 19: Mass distribution versus drop diameter compared to a log normal distribution with the same medium and mean mass size.

Oxidation and combustion

Table 3 shows the results of the gas samples taken at four locations, before the test and 5 minutes after blow-down. The variation of the samples regarding the position is small, which shows a good mixing of the containment atmosphere. At the end, about 3.3 % of hydrogen persists (dry basis). This makes an amount of about 2.2 % of the total gas, including vapor. The amount of hydrogen moles created by oxidation is estimated to be 27. This amount is consistent but a bit smaller than typical values for DISCO DCH experiments with steam blow-down (between 40 and 50 moles). This estimate is established with the nitrogen ratio method, which assumes that nitrogen is neither consumed nor produced by chemical reactions. In presence of vapor, oxidation of the melt with oxygen should be negligible.

The oxidation rates of iron can be estimated as follows:

- Oxidation rate considering the total Fe mass: 27 % if Fe is oxidized into FeO, 18 % if Fe_2O_3
- Oxidation rate considering the dispersed mass: ~ 100 % if FeO, 66 % if Fe_2O_3

This is very consistent with the DCH tests when relating the oxidation to the dispersed mass. Previous chemical analysis of the melt (DCH tests) showed that in fact, the oxidation occurs as Fe_2O_3.

Based on the consumption of oxygen, the estimated combustion rate is around 29 %. Compared to DCH tests, this is a small value. Indeed, in these DCH tests, it was estimated that all the produced hydrogen was burning as turbulent jets. The presence of water and very high amounts of vapor appear to limit strongly the combustion.

The theoretical value of pressurization due to combustion, for an adiabatic process is:

$$\Delta P_{H2} = n_{h2}\,(\gamma - 1)\frac{\Delta e_{H2}}{V}$$

where the term n_{H2} is the number of moles burned, γ is the adiabatic coefficient (around 1.36), Δe_{H2} is the reaction heat by mole and V is the volume. However, previous DCH tests led to a smaller pressurization, the origin of which was investigated but is still unknown. The results of the two estimates are as follows:

- Theoretical: $dP \sim 0.06.n_{h2} \sim 0.05$ MPa
- From previous DCH tests: $dP \sim 0.04.n_{h2} = 0.03$ MPa

The pressurization during the test (0.24 bars) indicates that the effective contribution is smaller. If the combustion was to occur lately and slowly in the upper part of the

containment vessel, then it should be affected by thermal losses, which would explain the small pressurization.
We might conclude that, although not negligible, the combustion during a FCI, in the absence of pre-existing hydrogen in the containment, has a relatively small impact on the pressurization.

Table 3: Measured gas concentrations of the test DISCO-FCI (dry gas measurement).

Time	**Location**	**Species (mole %)**		
		N_2	O_2	H_2
Pretest	Cont. low	79.24	20.76	0
	SubComp.	79.57	20.43	0.03
	Cont. high	79.42	20.58	0.03
	Cont. top	79.21	20.79	0.03
	Average	**79.36**	**20.64**	**0.02**
Posttest	Cont. low	77.42	19.17	3.41
	SubComp.	77.28	19.66	3.06
	Cont. high	77.22	19.29	3.49
	Cont. top	77.09	19.52	3.39
	Average	**77.25**	**19.41**	**3.34**

3.5 WP4 HYKA

In the case of a severe accident with and without failure of the reactor pressure vessel, the containment is the ultimate barrier to the environment. The HYKA facility provides unique research capabilities for investigation of hydrogen related phenomena in containment during severe accidents: hydrogen distribution, hydrogen combustion and hydrogen mitigation measures. In this work package phenomena are addressed that are ranked as *high priority issue by the SARP group of the SARNET NoE.*

HYKA offers new experimental possibilities for containment safety research in Europe through a number of large test vessels which are qualified and approved for operation with hydrogen combustion. The tests can be made under stagnant or under controlled air flow conditions, as well as in horizontal or vertical orientation. Due to the high vessel design pressures test parameters are not restricted by safety considerations. Highly energetic experiments can be performed on the KIT premises with all necessary infrastructure near-by (control rooms, data acquisition, gas preparation and filling systems, workshops).

In HYKA it is possible to investigate the whole spectrum of hydrogen phenomena. Research on different hydrogen sources and their distribution behaviour can be conducted, as well as experiments with different ignition sources. One of the most attractive features of HYKA is the capability for well-controlled, medium to large scale combustion experiments, covering all three combustion regimes (slow and fast deflagration and detonation). The main technical details of the different HYKA facilities are summarised in the Table 4.

An important outcome of the research activities in the DCH domain within SARNET was the understanding, that the combustion of hydrogen produced by oxidation during melt ejection from the RPV as well as the hydrogen initially present in the containment can be the dominant phenomenon for containment pressurization. It is now clear that the uncertainty in the combustion rate under these conditions was too large for the assessment of

containment integrity for certain reactors. Dedicated combustion codes (e. g. COM3D) are presently not capable to reproduce the results obtained in a first series of experiments with hydrogen release conducted in the DISCO facility at KIT. Moreover, the need for hydrogen combustion tests at a scale larger than 1:18 was stressed by the SARNET partners. Without those, the uncertainty in the extrapolation of experiments to reactor scale would still remain too large to assess the containment integrity for certain reactor geometries. This issue can be addressed in the experiments performed in the e.g. A2 vessel of the HYKA facility.

Three proposals had been received for use of 3 different vessels of the HYKA facility. Though only two experiments were originally planned in HYKA, the User Selection Panel expressed a great interest in all three of them. The panel strongly supported the KIT proposal to perform all three tests (with some adaptation of the HYKA-A3 vessel) since they all address the high priority SARP issues and therefore will contribute to the reduction of uncertainties in the hydrogen risk domain, and especially addressing scaling aspects will improve the accuracy of modeling.

Table 4: Technical details of the HYKA vessels.

Name	**Type**	**Dimensions (m)**	**Volume (m^3)**	**Design pressure (bar)**	**Potential experiments**
A 1	cylindrical vessel	diam. 3.4 length 12.0 (horizontal)	98	100	Large scale tests on turbulent combustion, flame acceleration, detonation, vented explosions
A 2	cylindrical vessel	diam 6.0 m length 10.5 m (vertical)	220	10	Large scale tests on turbulent combustion with mixture gradients, standing diffusion flames, vented explosions, interaction of recombiners with containment flows, test of deliberate ignition mitigation schemes
A 3	cylindrical vessel	diam. 2.5 length 8.0 (vertical)	33	60	hydrogen distribution, stratification, recombiner and igniter tests, uniform and non-uniform mixtures
A 6	cylindrical vessel	diam. 3.3 height 3.1	22	40	as A1, two large vents (0.8m) H_2 distribution in closed rooms, integrity of mechanical structures
A 8	cylindrical vessel	diam. 1.8 length 3.0 (horizontal)	9	100	fast deflagrations and detonations at high initial pressures
FTC	rectangular flow test chamber	8.5x5.5x3.3 airflow ≤ 24.000 m^3/h	160	1.07 static 1.7 dynamic	studies on vented combustions (up to 16 g H_2), testing of H_2 local detonations in closed spaces

The following experiments have been selected to be performed in the HYKA test facility:

Title: Detonations in partially confined layers of hydrogen-air mixtures (DETHYD)
Organisation: WUT, Warsaw, Poland

The experimental series were successfully completed in March 2011 i.e. in month 13 of the project with a minor delay of 2 months as compared to the original planning.

The aim of the experiments performed at HYKA facility in the A1 test vessel was to investigate critical layer thickness for hydrogen-air detonation propagation in semi-confined geometry. Semi-confined combustion scenarios are very important from practical point of view because light, flammable gas released in confinement will accumulate at the top of the room. These phenomena may take place in containments of nuclear reactors or in tunnels. When detonation propagates in smooth tube, the critical tube diameter d* is in a relation with detonation cell size λ: $d^* \cong \lambda$. Critical thickness h^* and its relationship with λ for semi-open geometry is unknown.

In the experiments a rectangular 3 x 9 m channel with various gas layer thicknesses of 8, 5, 3 and 2 cm was used. The hydrogen-air mixture layer thickness was controlled by thick (10 μm) plastic film. The geometry was placed in cylindrical 100 m^3 safety vessel as shown in Fig. 20 and Fig. 21.

To assure uniform flame and detonation front special “linear ignition device” with exploding wire and 60 cm length acceleration section were developed. Due to the acceleration section run-up distance for detonation was lower than 1 m. Instrumentation was composed of 15 dynamic pressure transducers (13 at the top – along the ceiling symmetry line, 2 on the ground), 20 ionization sensors and 48 sooted plates (40 in test section, 8 in “booster”). The sooted plates were used to indicate detonation propagation range in the test layer.

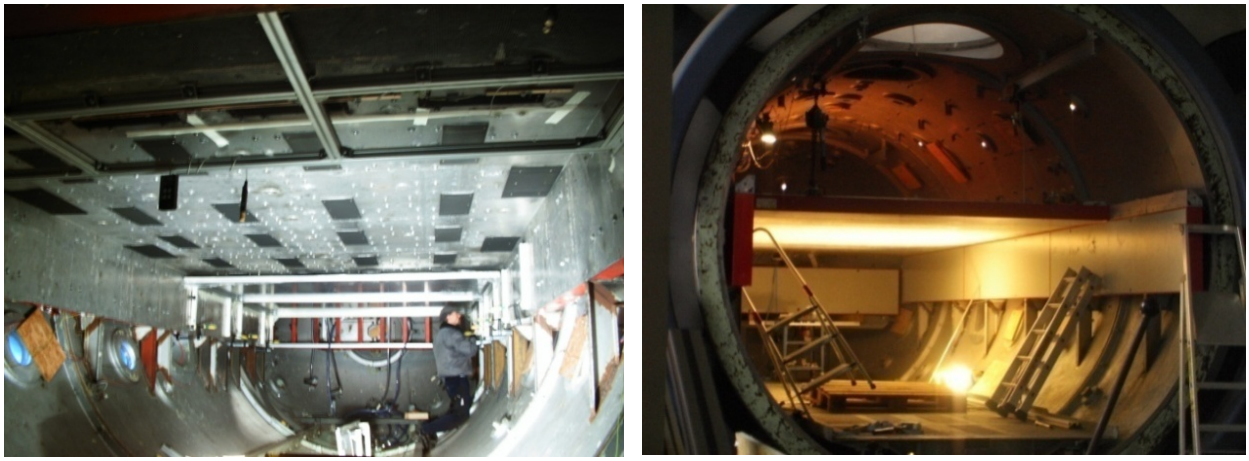

Fig. 20: The investigated geometry placed in safety vessel (sooted plates visible at the ceiling – left side picture).

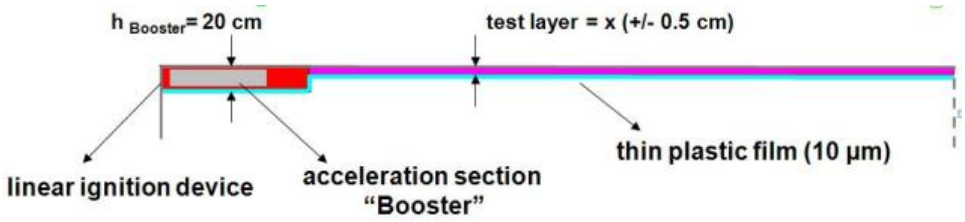

Fig. 21: Cross-section of the investigated geometry.

The conducted experiments show that critical thickness h^* of flammable hydrogen-air mixture is equal to 3 cm (see
Table 5), which corresponds to the relation with detonation cell size λ: $h^* \approx 3\lambda$. In one case with 3 cm layer thickness detonation attenuation was recorded at the distance lower than 2 m. At the second test for 3 cm layer thickness detonation propagates up to the end of the tested geometry. For 2 cm layer, detonation was suppressed at the distance lower than 1 m.

Table 5: Main results of performed experiments.

Test #	% H_2	Layer thickness [cm]	Detonation propagation?	Detonation range in test layer (specified by sooted plates)
1	30	8	Yes	Up to the end
2	30	5	Yes	Up to the end
3	30	3	No	< 2 m
4	30	3	Yes	Up to the end
5	30	2	No	< 1 m

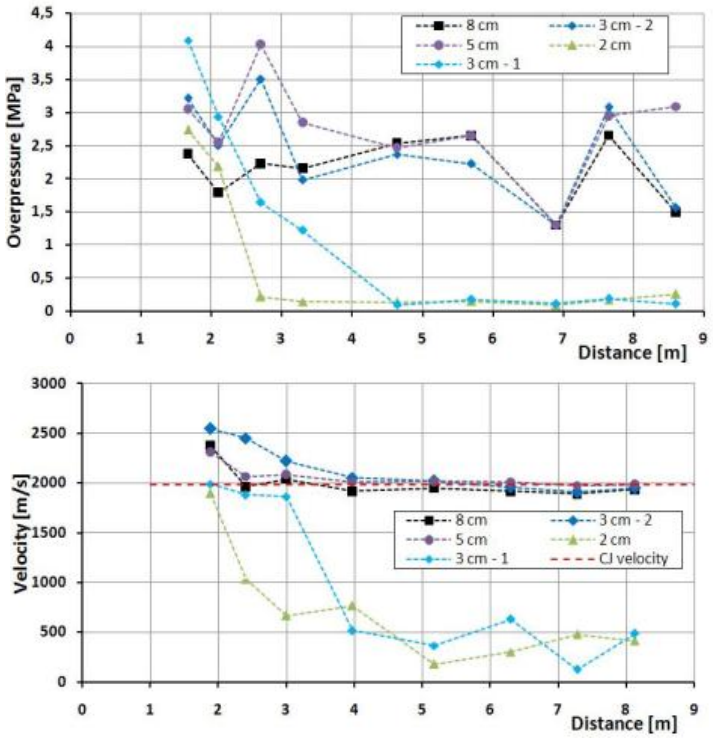

Fig. 22: Overpressures and velocities for different layer thickness.

Recorded pressures and velocities (Fig. 22) confirm that for 2 cm and 3 cm (test 1) layer thickness detonation attenuation occurs. For these cases detonation propagation ranges are in accordance with sooted plates indications. After detonation, attenuation velocities vary in the range of 150 - 600 m/s, overpressures are in the range of 0.1 – 0.25 MPa which corresponds to the fast deflagration regime. For the cases with detonation present up to the end of the geometry, overpressures are in range of 1.3 – 3.1 MPa and velocities are ~ 2000 m/s, which corresponds to the stable C-J detonation regime.

Joint paper on the results of the HYKA-DETHYD experiments was presented at the ERMSAR-2012 Conference in March 2012.

Title: Hydrogen concentration gradients effects understanding and modelling with data from experiments at HYKA (HYGRADE)
Organisation: CEA, Saclay, France

The experimental campaign, including facility reconstruction, preliminary “cold” experiments to create proper hydrogen concentration gradient and main part with combustion experiments, takes time from 28.08.11 to 13.03.12. Therefore the experimental campaign started in month 19 of the project with 2 months delay as compared to the original planning caused by a serious reconstruction of the A3 vessel.

Background
During certain postulated accidents in a nuclear reactor containment, hydrogen gas can be released into the reactor building. Depending on the local concentration and/or presence and activation of mitigation devices, hydrogen may burn following different combustion regimes. These regimes may include jet fires, slow deflagrations, fast deflagrations and detonations depending on the combustion process development. Thus, one has to estimate the severity of a combustion process under given geometrical configuration, scale, and composition of combustible mixture. These data then can be used in structural mechanics analysis codes to verify the integrity of the structure.
Experimental details
Experiments are performed inside the A3 cylindrical vessel (Fig. 23, left) of 8 m total height and 2.35 m of internal diameter. The facility, having total volume of 32.8 m^3, consists of two chambers, lower (21.6 m^3) and upper (11.2 m^3), separated by round duplex door of 1 m diameter. During the experiments the door between compartments was removed. Internal structures comprise the supporting metal frame and the obstacles made of plywood (Fig. 23, right).

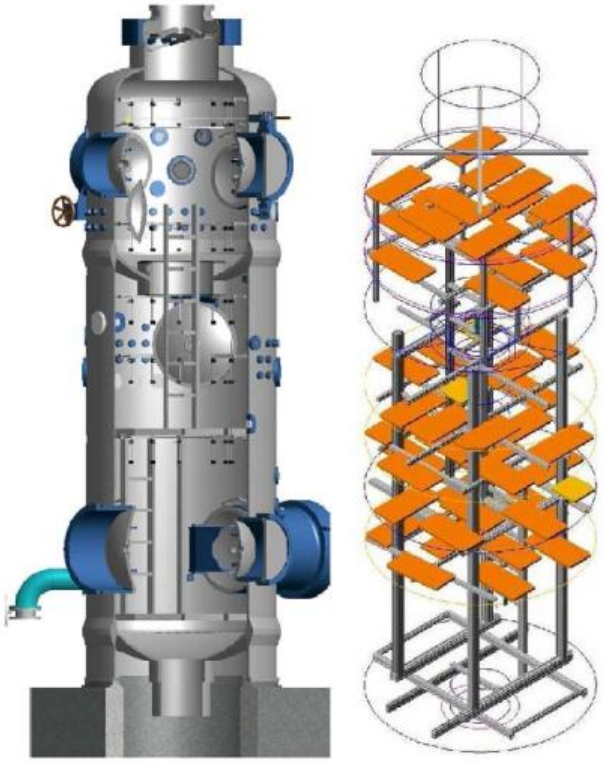

Fig. 23: General view (left) of the A3 facility and internal structures (right) used for experiments.

There are six layers of obstacles of BR[2] ≈ 40 % and the annular compartments separating surface of BR ≈80 %. Eight dynamic pressure sensors are installed inside A3 facility, and flame detection is performed using 16 thermocouples located approximately along the axis of symmetry, and 44 ionisation probes. 49 gas sample probes (volume of each = 16 ml) are installed inside the A3 facility at different levels and positions in order to measure the light gas concentration in the vessel. The valve opening is time controlled, and the filling time of a sample volume is less than 1 second. The gas concentration is measured afterwards in specific heat conductivity column. Since the experiments investigate hydrogen deflagration in presence of longitudinal hydrogen concentration gradients, a special procedure to create a positive and negative concentration gradient with respect to gravity was developed.

Gradient formation procedure

Gradient formation inside the A3 vessel is performed using three injection lines: horizontal line at the bottom, horizontal line at the top, and vertical line positioned along the vertical axis of symmetry (Fig. 24). Injection lines at the top and at the bottom are built as double rings fitted with large quantity of nozzles (d = 2.2 mm), while the vertical line at the axial position is designed to produce four symmetrical horizontal jets per level with decaying nozzle size from top to bottom (from 5.5 mm down to 2.2 mm in 0.1 mm steps). A 4 m^3 gas storage tank is connected with automatic valves to the three injection lines. Three electric fans are installed inside, one in the smaller upper chamber, and the other two in the lower larger chamber. The procedure for gas mixing consisted of two steps:

- Step (1): creation of a homogeneous mixture in the vessel. Initially the pressure inside the light-gas-storage tank is P_0 = 6 bar. The gas is simultaneously injected at the top and at the bottom of the vessel through the corresponding top and bottom horizontal

[2] BR = Blockage Ratio, that means the ratio of blocked cross-section to total cross-section of the volume

lines, until the pressure inside the storage tank reaches a predetermined boundary value. After the injection the gas in the vessel is mixed during 8 minutes by the three fans. Two minutes later the homogeneous mixture is prepared.

- Step (2): creation of a concentration gradient in the vessel. Considering an example of the filling process, injection of 0.1 m^3 of light gas at the top of the vessel (which corresponds to 25 mbar pressure decay in the tank) is directly followed by the main injection using the vertical axial line. Gas sampling starts 30 s after the last injection, the overpressure in the vessel A3 is 50 mbar in this case. Two examples of “positive” and “negative” hydrogen concentration gradients used in current work are shown in Fig. 25.

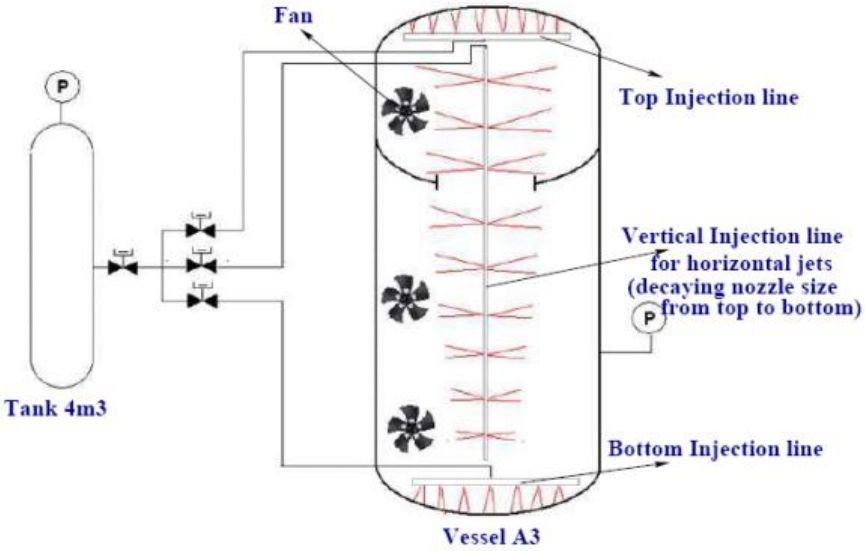

Fig. 24: Sketch of the facility and instrumentation used for concentration gradient formation.

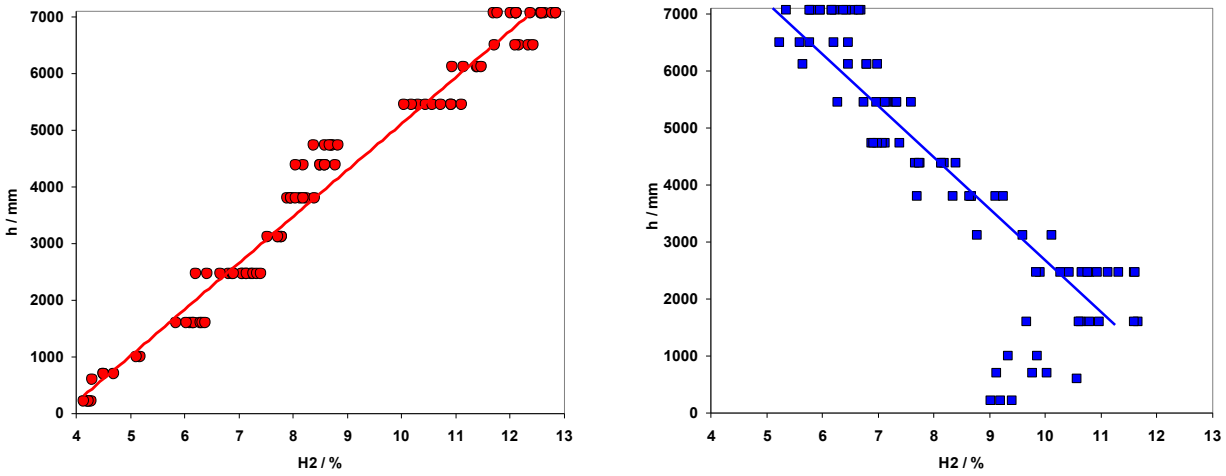

Fig. 25: Example of experimental concentration gradient. The lower part of the concentration gradient is modified in the case of a negative gradient.

Experimental data analysis

There are ten tests in total performed inside A3 facility (Table 6): three tests with homogeneous hydrogen concentration, three tests with hydrogen concentrations having negative slopes and lower ignition (at 1.2 m), two tests with hydrogen concentrations having positive slopes and upper ignition (at 7.078 m).

Table 6: Initial conditions for the experiments.

Test Description	H_2 Concentration (Vol.%)	Ignition Pos. (m)	P_0 (bar)	T_0 (K)	Unburned (Vol.%)
Test 3, homog.	9.04	1.2	1.037	278.25	0.08
Test 4, negat.	$12 \rightarrow 6$	1.2	1.086	277.65	0.59
Test 5, negat.	$12.8 \rightarrow 6.8$	1.2	1.08	278.45	0.17
Test 6, negat.	$13.3 \rightarrow 7.3$	1.2	1.08	277.55	0.07
Test 7, posit.	$4 \rightarrow 12$	0.2	???	281.75	0.49
Test 8, posit.	$4 \rightarrow 12$	7.078	1.075	282.75	1.25
Test 9, posit.	$6 \rightarrow 13.3$	0.02	1.105	286.35	0.16
Test 10, posit.	$5 \rightarrow 13.3$	7.078	1.095	290.25	0.4

The results of experiments is divided into three parts: description of results corresponding to the Test 3 (homogeneous concentration); description of results corresponding to the Tests 4-6 (negative gradient concentration), and description of results corresponding to the Tests 7-10 (positive gradient concentration). For each test with non-homogeneous hydrogen gas initial concentration, the equivalent averaged hydrogen concentration, which, together with initial pressure and temperature the asymptotic AICC (Adiabatic Isochoric Complete Combustion) state for overpressure was computed. These theoretical values are systematically compared with the corresponding maximum experimentally measured overpressures. Flame time-of-arrival diagrams as well as the average flame velocity deduced from adjacent thermocouples are represented for each Test.

Tests with initially homogeneous concentrations

Three tests were performed in A3 with initially homogeneous mixture of hydrogen gas and air. Here we present and analyze the result of the Test 3. The corresponding initial conditions are the following: P_0 = 1.037 bar; T_0 = 278.25 K; X_{H2} = 9.04 %. Based on the above initial conditions we can compute the asymptotic AICC (Adiabatic Iscochoric Complete Combustion) state. The results for pressure and temperature given by CHEMKIN code are P_{AICC} = 4.386 bar; T_{AICC} = 1233.0 K, meaning that the maximum achievable final overpressure for this test cannot exceed 3.349 bar.

Experimentally measured pressure evolutions by different transducers are presented in Fig. 26, left. For this test, like for all the other tests, the overpressure evolution measured by the pressure transducer PC8 (Z = 7.47 m) is always lower than the corresponding overpressure values measured by the other transducers. For the purpose of comparison we shall always use the overpressure evolution corresponding to the highest values. The maximum pressure level reached (taking data from transducer PC1) is 2.43 bar, which is 27.44 % relatively lower than the ΔP_{AICC} pressure corresponding to 3.349 bar. Taking into account the fact that only negligible part of hydrogen gas is left after the combustion process (0.8 %), one can make a conclusion that the insufficient pressure level is due to energy losses. Overpressure evolution (data taken from transducer PC1) shows almost linear behavior from 0.3 bar up to 1.2 bar, and the approximate slope is dp/dt = 4.25 bar/s.

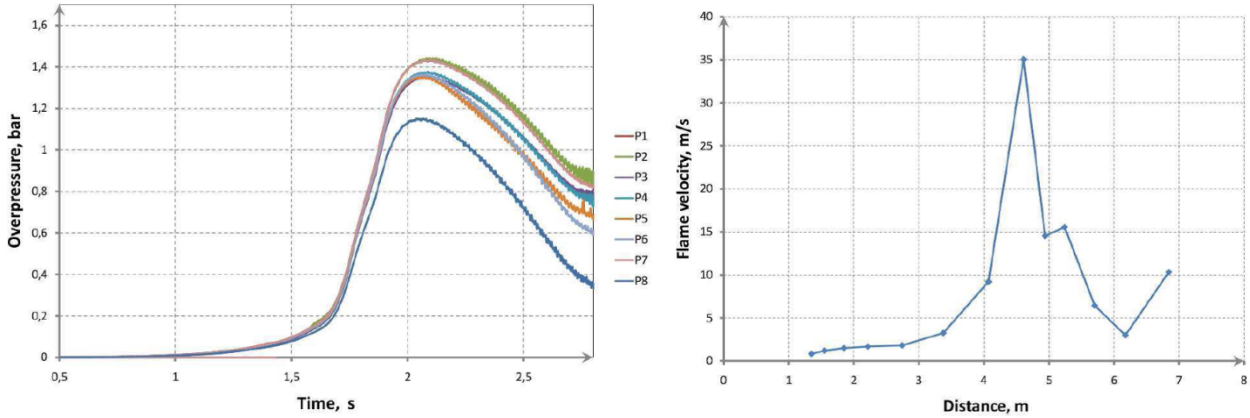

Fig. 26: Homogeneous concentration. Experimentally measured pressure for different transducers (left) and flame velocity along the axis of symmetry (right). Data points are taken from thermocouples TC01-TC16.

The flame evolution along the curve close to the centerline position is given in Fig. 26, right. Initially, the flame has a very low velocity, of the order of 2-5 m/s. It accelerates up to 35 m/s when the BR increases (through the door connecting the compartments, Z = 4.7 m), and decelerates after, oscillating between 3 and 15 m/s.

Tests with negative hydrogen concentration gradient

Three tests were performed with negative gradient initial hydrogen concentrations in air (see Test 4, Test 5 and Test 6 in Table 6). As in the previous test we compute AICC overpressure based on averaged initial hydrogen concentration. These results, as well as the experimentally measured maximum overpressure levels are summarized in Table 7. The hydrogen molar fraction is taken as uniform and equal to 10 % at the lower part of the facility, 0 < Z < 1 m due to uncertainties.

Table 7: Averaged hydrogen concentration, hydrogen mass, and ΔP_{AICC} overpressure.

Test	$\overline{X}_{H_2}$ (%)	m_{H_2} (kg)	$\triangle P_{AICC}$ (bar)	$\triangle P_{exp}^{max}$ (bar)	Err_{rel} (%)
T4_NEG_12.0-6.0%	9.08	0.258	3.529	2.616	25.87
T5_NEG_12.8-6.8%	9.768	0.276	3.7244	3.06	17.83
T6_NEG_13.3-7.3%	10.12	0.288	3.813	3.66	4.01

The experimentally measured pressure evolutions for each test are presented in Fig. 27, left. The overpressure measured by the transducer PC8, as in the homogeneous test, is generally lower for all three tests. All the other pressure curves show similar behavior until the end of the combustion process; soon after the overpressure levels reach maximum values the curves start to diverge.

We can see that the peak overpressure level increases with averaged concentration. The comparisons of the pressure evolutions corresponding to three tests (Fig. 27, left) show that by increasing the averaged concentration level we increase overpressure peak by 0.5 −0.6 bar. The pressure curves experience almost linear behavior when the rate of pressure increase is the highest, i.e. from 0.5 bar up to1.5 bar. Again, the slope increases, from 60.58 bar/s up to 130.65 bar/s with increasing averaged concentration and the local concentration at the ignition position. Looking at the Table 7 we can see that the relative difference between the maximum experimental overpressure and the theoretical ΔP_{AICC} overpressure decreases with increasing averaged concentration.

Flame velocities computed using the data from the adjacent thermocouples show oscillatory behavior (Fig. 27, right): flame accelerates when the gas flow ahead contracts due to presence of obstacles, and the highest velocity (530 m/s) is reached at the place with the highest blockage ratio, i.e. when the flame penetrates into the upper part of the facility. Higher averaged and local initial hydrogen concentration leads to the higher visible flame velocity; for the lowest concentration (Test 4) flame velocity does not even exceed the speed of sound in the fresh mixture, while for the other two tests the visible flame speed during some parts of the trajectory either has the similar values or exceeds the velocity of sound.

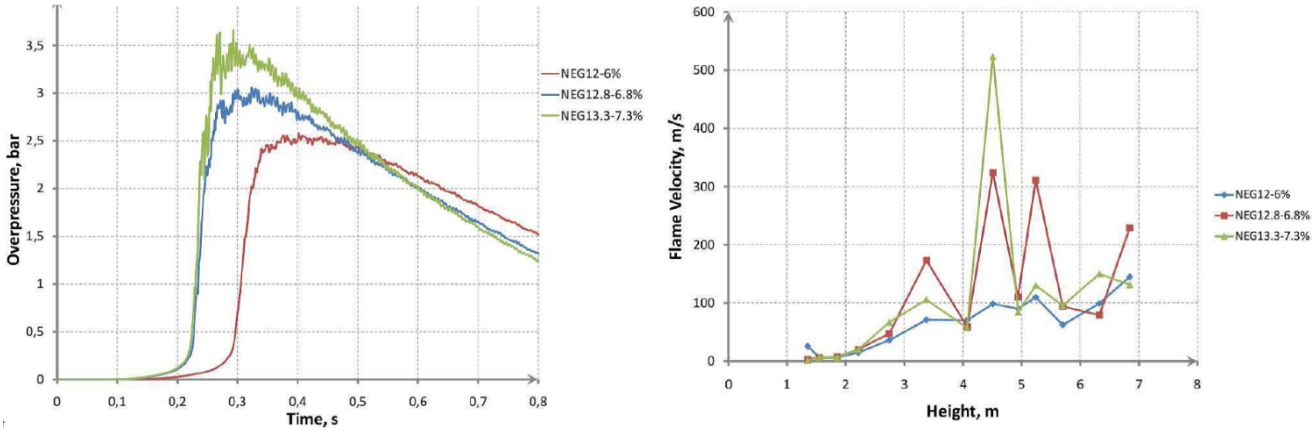

Fig. 27: Negative gradient concentrations. Pressure records (left) and flame velocity along the axis of symmetry (right) corresponding to test 4 (blue), test 5 (red), and test 6 (green).

Tests with positive hydrogen concentration gradient

Four tests were performed with positive gradient initial concentrations (see Test 7, Test 8, Test 9, and Test 10 in Table 8). The ignition position varied for these tests, i.e. for two tests (7 and 9) the hydrogen-air mixture was ignited at 0.2 m and 0.02 m, respectively, while for the other two tests (8 and 10) it was ignited at 7.078 m. This implies that in the former case the mixture was ignited at the low hydrogen concentration location, and in the latter case at the relatively high hydrogen concentration location. This leads to big differences in the results, as is shown below. We compute AICC overpressure based on averaged initial hydrogen concentration. These results, as well as the experimentally measured maximum overpressure levels are summarized in Table 8.

Table 8: Averaged hydrogen concentration, hydrogen mass and AICC overpressure corresponding to Tests 7-10.

Test	Ignition Pos. (m)	$\overline{X}_{H_2}$ (%)	m_{H_2} (kg)	$\triangle P_{AICC}$ (bar)	$\triangle P_{exp}^{max}$ (bar)	Err_{rel} (%)
T7_POS_4.0-12.0%	0.2	8.19	0.226	3.145	2.187	30.46
T8_POS_4.0-12.0%	7.078	8.19	0.226	3.133	2.75	12.23
T9_POS_6.0-13.3%	0.02	9.83	0.275	3.72	2.85	23.39
T10_POS_5.0-13.3%	7.078	9.35	0.256	3.618	3.514	2.99

The experimentally measured pressure evolutions for each test are presented in Fig. 28. The overpressure measured by the transducer PC8, as in the previous tests, is generally lower for all present tests. All the other pressure curves show similar behavior until the end of the combustion process; soon after the overpressure levels reach maximum values the curves start to diverge. The pressure signals, corresponding to the tests where the mixture was ignited at the low hydrogen concentration end (tests 7 and 9), show comparatively

smooth character compared to the signals corresponding to the upper ignition tests (tests 8 and 10). For the latter case, high-amplitude oscillations start to develop when the overpressure is close to its maximum. We attribute such behavior to the influence of weak shock waves (sometimes called “acoustic waves”). The mixtures ignited at the low concentration limit produce low-amplitude shock waves, which are easily damped by the internal structure.

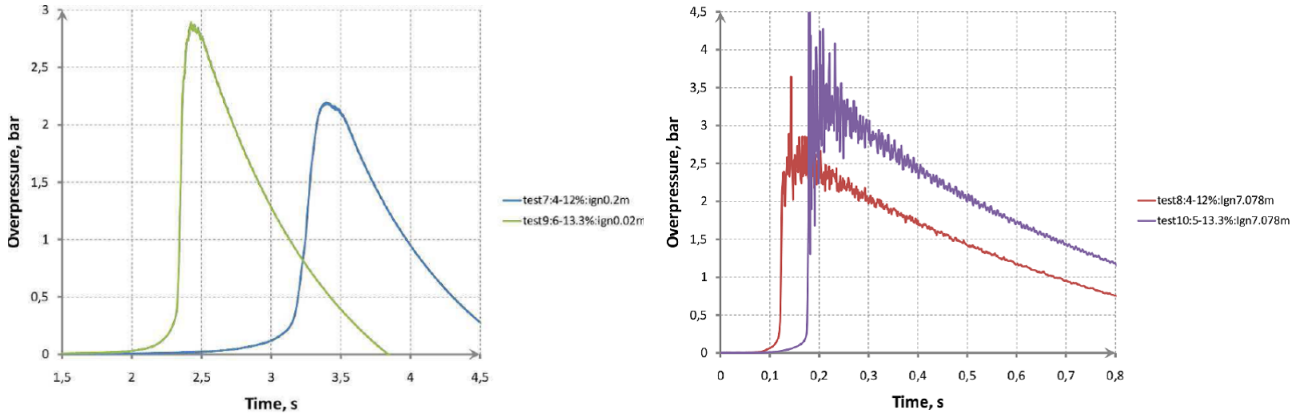

Fig. 28: Experimentally measured pressure from transducer P1; tests 7, 9 (left) and tests 8, 10 (right).

Due to the analysis, it was found that the maximum overpressure level depends strongly on ignition location: ignition at the place where the hydrogen concentration is higher leads to higher final overpressure. Another observation was that the time period between the ignition and the moment of highest pressure increase rate differs considerably between two groups; it is approximately 2.3 s and 3.2 s for the first group, and 0.12 - 0.17 s for the second group. This time delay is a function of initial flame development, which strongly depends on the hydrogen concentration at the ignition location.
The pressure curves experience almost linear behavior when the rate of pressure increase is the highest, i.e. approximately from 0.5 bar up to 1.5 bar. The slope dP/dt has highest values for the Tests 8 (515 bar/s) and 10 (970), i.e. when the mixture is ignited at the higher hydrogen concentration. At the same moment the pressure rate values for low concentration ignition is much smaller, 11 bar/s for the Test 7 and 51 bar/s for the test 9.

Flame velocities (Table 9) computed using the data from the adjacent thermocouples show oscillatory behavior. For bottom-ignited tests 7 and 9 flame velocity gradually increases up to the connecting door between the chambers, where it experiences strong acceleration and deceleration. For top-ignited tests 8 and 10 strong acceleration-deceleration is observed at almost every layer of obstacles, and velocities reached are several times higher (in absolute terms) than the one reached for the tests 7 and 9. As for the negative gradient concentrations tests, higher averaged and local initial hydrogen concentration generally leads to the higher visible flame velocity.

Table 9: Values for speed of sound in combustion products at ignition a_{cp_ign}, expansion ratio at ignition σ_{ign}, expansion ratio based on averaged hydrogen molar fraction σ_{aver}, expansion ratio gradient $d\sigma/dx$ and maximum flame velocity V_{max} for the non-homogeneous tests.

Test description	$a_{cp-ig.}$ (m/s)	σ_{ign}	$\sigma_{aver.}$	$d\sigma/dx$ (1/m)	V_{max} (m/s)
T4_NEG_12.0-6.0%	699.72	4.15	3.45	−0.256	109.8
T5_NEG_12.8-6.8%	717.31	4.33	3.61	−0.251	323.81
T6_NEG_13.3-7.3%	727.79	4.45	3.7	−0.25	523.1
T7_POS_4.0-12.0%	493.24	2.12	3.19	0.292	97.0
T8_POS_4.0-12.0%	700.93	4.09	3.19	−0.292	620.0
T9_POS_6.0-13.3%	554.51	2.61	3.55	0.254	130.0
T10_POS_5.0-13.3%	730.64	4.29	3.4	−0.288	750.0

Title: Upward flame propagation experiment in air-steam-hydrogen atmosphere (UFPE)
Organisation: JSI, Ljubljana, Slovenia

The Reactor Engineering Division of the Jozef Stefan Institute (JSI) from Slovenia submitted a proposal for an experiment on hydrogen combustion in the HYKA A2 experimental facility in April 2010. The title of the proposed experiment was Upward Flame Propagation Experiment (UFPE). The proposal was subsequently reviewed by independent experts and accepted by KIT in the fall of 2010. The UFPE experiment was not foreseen in the original LACOMECO planning and was executed additionally according to the proposed specification on March 12, 2012.

Physical background and motivation
During a hypothetical severe accident in a pressurized water reactor (PWR) nuclear power plant, hydrogen would presumably be generated during the degradation of the reactor core. Hydrogen would flow into the plant containment and, due to its low density, gather in the upper parts of the containment, thus creating a region in which local hydrogen concentration could be sufficiently high for the mixture of air, steam and hydrogen to be flammable. The ignition and ensuing combustion of hydrogen could cause a sharp pressure increase which could threaten the integrity of the containment.

Experiments on hydrogen combustion (specifically, hydrogen deflagration) are being performed to gain knowledge about this phenomenon, so that the magnitudes of the consequences of hydrogen combustion during a hypothetical accident in an actual nuclear power plant could be assessed as accurately as possible. Different experimental facilities are used, from simple tubes (such as the ENACCEF facility, located at the ICARE centre of the Centre National de la Recherche Scientifique in Orléans, France) to vessels assuming the shape (but not the volume) of actual containments (such as the THAI facility at Becker Technologies GmbH in Eschborn, Germany). These experimental facilities are necessarily scaled-down, compared to the containments of actual nuclear power plants. Experimental results obtained in facilities are used to gain knowledge about the phenomena that would presumably occur in actual plants.

Table 10: Main dimensions and scaling factors for typical nuclear reactor containment and experimental facilities.

Dimension	US APWR	HYKA-A2	THAI	US APWR	HYKA-A2	THAI
	Dimension values			Dimensionless values (THAI = 1)		
Total volume, m^3	125000	220	60	2100	3.7	1
Integral scale $V^{1/3}$, m	50	6	3.9	12.8	1.5	1
Diameter, m	50	6	3.2	15.6	1.9	1
Height, m	63	9.1	9	7	1	1
Aspect ratio, H/D	1.3	1.5	2.8	-	-	-

A similarity of the reactor containment geometry and experimental facilities is also one of important requirements to the experimental scaling procedure. Fig. 29 shows a relative aspect ratio of one of the PWR designs in comparison with two experimental facilities to be used for the scaling experiments. A US APWR reactor and THAI and HYKA-A2 facilities were chosen as most representative for the scaling analysis. A comparison of scales as a ratio of linear dimensions or cube roots of volumes is given in Table 10 for real and experimental volumes. In general, these three objects as APWR containment, HYKA-A2 and THAI facilities are related as 13**:**1.5**:**1 in terms of scale. They have aspect ratios 1.3**:**1.5**:**2.8. Therefore, the HYKA-A2 vessel has almost the same aspect ratio as US APWR containment with almost 8 times scale difference. This might be a very important issue for the experimental scaling of combustion processes.

From the point of view of nuclear safety, this evaluation of possible actual consequences based on experimental results is somewhat uncertain. The following issues are still open:

- If experiments are performed at similar (qualitative) experimental conditions, would the resulting phenomenon of hydrogen combustion change continuously, or could a change to a completely different behaviour occur?
- Can phenomena observed in a scaled-down experimental facility be extrapolated to an actual containment, and, if yes, how should that extrapolation be done?

Thus, performing more experiments on hydrogen combustion at completely different experimental conditions, which were not considered yet, would not necessarily contribute to nuclear safety, if the two above-mentioned issues are not sufficiently clarified. Therefore, the basic principle, when devising the proposal for the experiment, was to consolidate already existing knowledge. It was proposed to perform an experiment, which would not be very different from experiments already performed in other experimental facilities, and would be somewhat complementary to them.

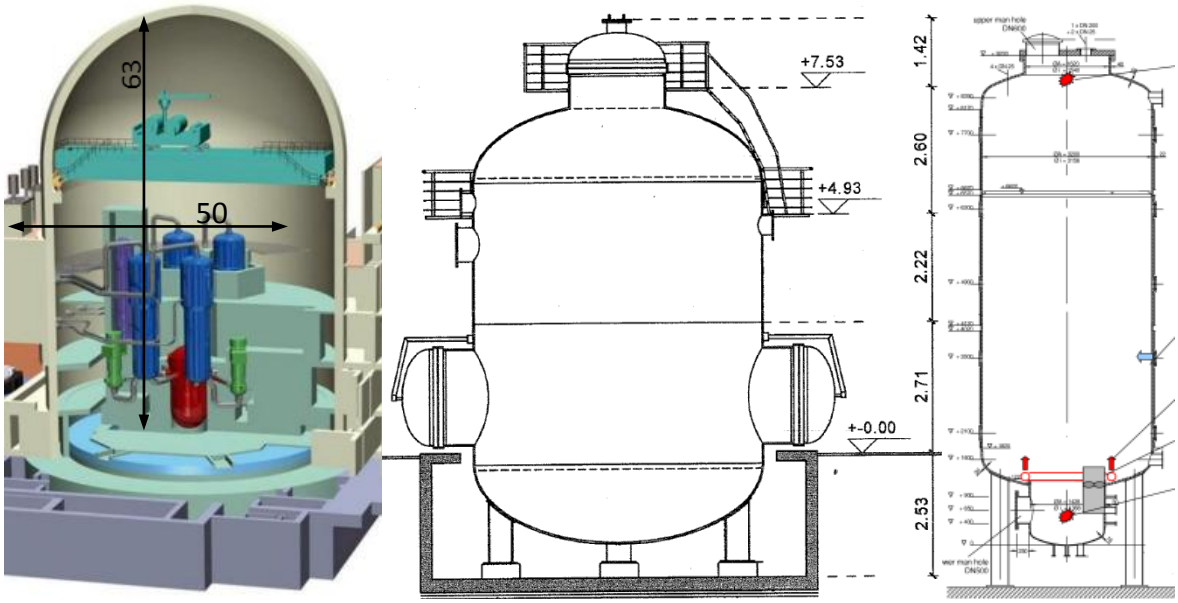

(a) APWR (b) HYKA-A2 (c) THAI

Fig. 29: A comparison of main dimensions of nuclear reactor containment and experimental facilities: (a) US APWR; (b) HYKA-A2; (c) THAI.

Outline of the UFPE experiment and test parameters

JSI proposed to perform the UFPE experiment in the HYKA A2 test facility. The experiment should be performed similar to the experiment THAI HD-22, in which hydrogen deflagration was observed. The internal volume of the THAI vessel is 60 m^3, with an internal height of 9.2 m, and with the diameter of the main cylindrical part equal to 3.2 m. For the hydrogen combustion experiments, internal structures were removed from the interior of the vessel, so that an empty single compartment was obtained. The experiment THAI HD-22 was also used in the OECD International Standard Problem No.49 on hydrogen combustion, which was organized in 2009 and 2010.

For the UFPE experiment, the volume of the HYKA A2 test facility is 220 m^3. The inner height is 9.1 m, whereas the inner diameter is 6.0 m. Thus, although the volume of the facility is more than 3 times the volume of the THAI vessel, the heights are of the same order. The UFPE experiment was supposed to provide the information about the influence of the widening of the vessel on the flame behaviour. This could be used to infer the behaviour of the flame in an actual containment, where this phenomenon would have to be extrapolated even further.

In the hydrogen combustion experiment THAI HD-22, air, steam and hydrogen were initially present in the vessel atmosphere. The initial pressure was 1.5 bar, the initial temperature was 90 °C, the initial steam concentration was 25 vol%, and the initial hydrogen concentration was 10 vol%. The flame propagated from the bottom of the vessel in the upward direction, and in the radial direction towards the vessel cylindrical wall. During the experiment, the maximum pressure was about 5 bar, whereas the maximum temperature was about 900 - 930 °C. The spatial flame structure at different times, based on thermocouple measurements, was graphically presented as isochrones of flame positions. The average flame velocity at the vessel axis was about 2.9 m/s. Locally, close to the upper part of the facility, velocity increases up to 5.5 m/s. The integral characteristics of the HD-22 experiment as maximum combustion pressure and temperature of combustion are in good

agreement with thermodynamic calculations. There is some deficit of maximum combustion pressure and temperature compared to thermodynamic combustion characteristics T_{iacc} and P_{iacc}. The reasons could be an incomplete hydrogen combustion and energy losses to sidewalls.

The main purpose of the UFPE experiment would be to investigate the influence of a larger scale of the combustion vessel A2 on qualitative and quantitative differences, by comparing the results to experimental data obtained in a smaller vessel, like THAI-facility. The experimental data are also required to be used as benchmark experiments for CFD-codes and lamped-parameter codes validation of large scale numerical simulations of hydrogen deflagration.

Experimental details

The volume of the HYKA A2 test facility, as prepared for the UFPE experiment, is 220 m^3. The inner height is 9.1 m, whereas the inner diameter is 6.0 m. Fig. 30, left shows a photograph of the facility with an external thermal isolation. Fig. 30, right shows part of the facility blueprint with main dimensions to be used for numerical simulations. A floor made of planks was installed at the level of 420 mm from lower point to isolate the vessel from the sump region. The ignition device is located at level 1500 mm above the floor.

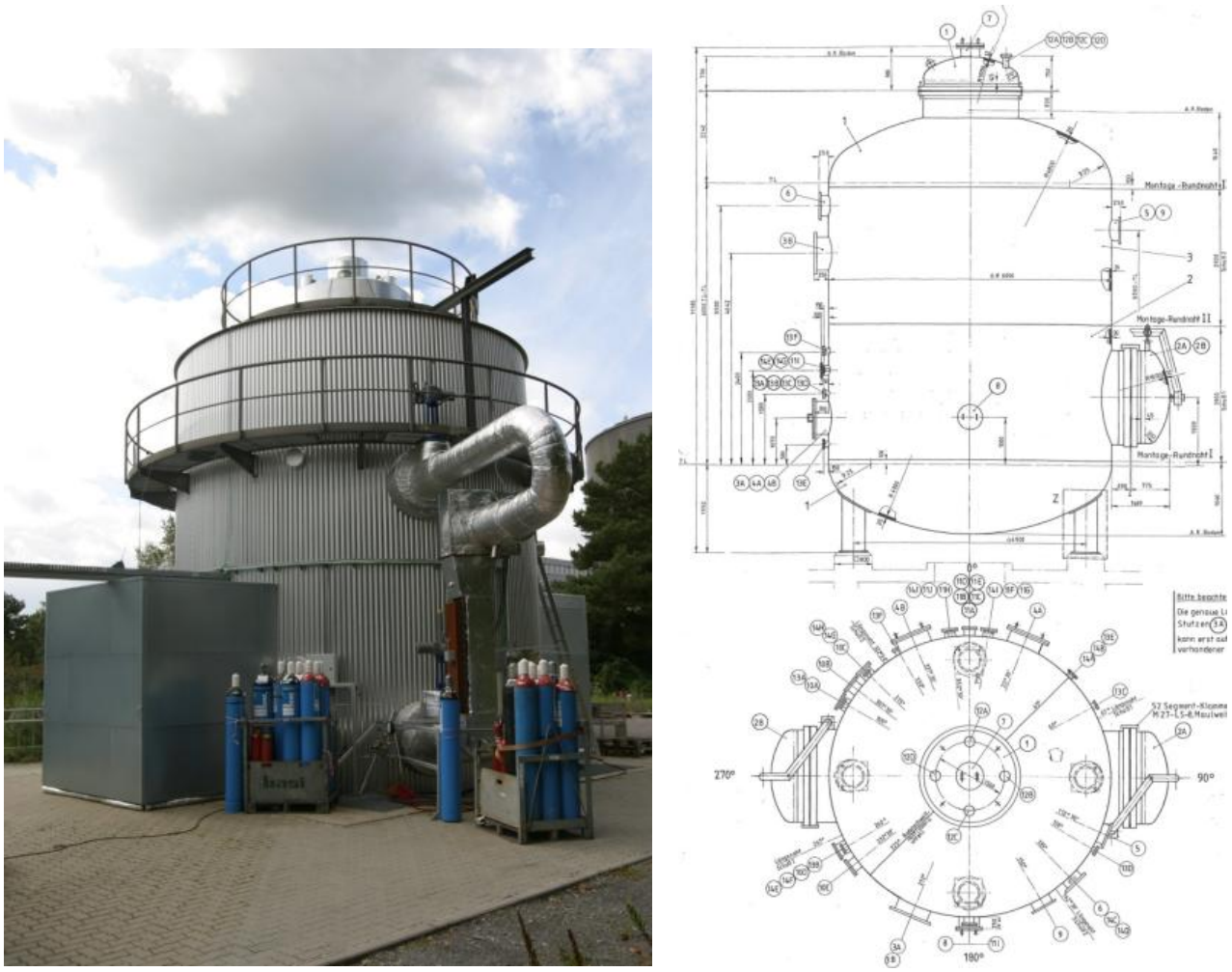

Fig. 30: HYKA-A2 facility in operational state with thermal isolation (left);
HYKA-A2 facility blueprint (right).

Several principal measures have been done to provide the required experimental conditions. The vessel was equipped with gas filling system including steam-generator and heating system. The gas filling procedure was the following: (1) preparing of dry hydrogen-air mixture; (2) heating up to the temperature 90 °C; steam injection up to the pressure P = 1.5 bar. Sampling probes method was used to control uniformity of the mixture before experiments. 6 sampling points were chosen to measure the mixture composition before and after the test. 33 thermocouples were installed inside and outside the A2 vessel to record local combustion temperature and to control thermal uniformity of the mixture. Additional purpose to use the thermocouples inside the vessel was to register flame arrival time at certain thermocouple positions. 4 fast PCB (piezoelectric type of pressure sensors) pressure sensors together with 2 Kistler and 4 Kulite sensors have been mounted on the internal wall to measure the absolute combustion pressure and dynamics of combustion in terms of dP/dt. 2 slow pressure sensors have been used to measure quasi-static pressure during the gas filling procedure before the test and quasi-static combustion pressure during the gas filling procedure before the test and quasi-static combustion pressure during the combustion test.

The high speed shadow photo (Background Oriented Schlieren technique) combined with pressure sensors (piezoelectric type of pressure sensors), and thermocouples were used to register dynamics of hydrogen combustion. A stochastic black-white background pattern was painted directly on the walls inside the vessel. A normal Canon-camera, three high speed cameras (Photron and Olympus), a normal Sony video-camera used to record top view and side view of flame development. The data acquisition system with 1 MHz sampling rate was used to record pressure, and temperature signals. The result was a pressure- or temperature signal-time history. Post processing of BOS (Background Oriented Schlieren technique) images was required to visualize flame shape and its position. Fig. 31 shows the arrangement of measurement system of HYKA-A2 vessel for UFPE experiments.

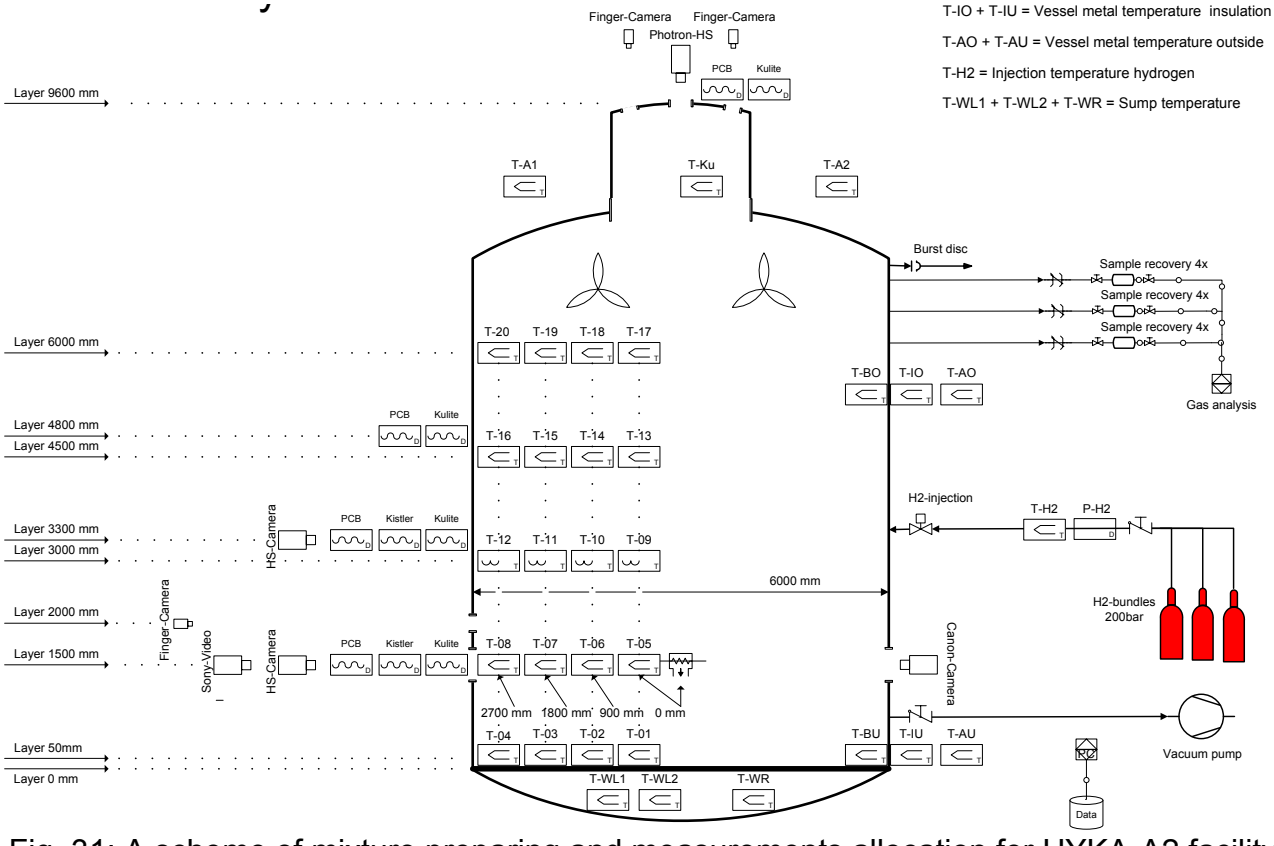

Fig. 31: A scheme of mixture preparing and measurements allocation for HYKA-A2 facility.

Two experiments were performed in the A2 vessel of HYKA of the IKET test side in order to study upward propagation. In order to approach to the THAI experiment HD-22 the hydrogen-air-steam mixture was prepared inside the A2 vessel: pressure 1.5 bar; temperature 90 °C; 12 % hydrogen/air mixture with 20 % of steam; lower ignition position h = 1.5 above the floor (Fig. 31). The test mixtures were prepared *in situ*, directly inside the vessel A2, by a partial pressure method. The procedure was the following: To the air at atmospheric pressure, which was heated up to temperature 90 °C, the hot steam at 90 °C was injected up to the total pressure 1.35 bar. Then hydrogen at 90 °C was injected up to the final pressure 1.5 bar. Two fans were installed at the top of vessel to mix the gaseous composition. The mixture uniformity was controlled by sampling probe method taken from six different points. The accuracy of measured concentrations was within the limit ± 0.15 %. The fans were switched off at least 3 minutes before the ignition moment to be enough to completely suppress the turbulence produced by fans.

Experimental results and analysis

Since hydrogen flame is practically invisible, the post processing using BOS technique was performed to monitor flame shape and its position. Fig. 32 shows the initial stage of flame development from an ignition moment until a mushroom – shape of combustion zone was generated due to buoyancy effect. The flame shape demonstrates a dominant upward flame propagation. The linear flame velocity was changed from 1 to 5 m/s with an average value of 2.8 m/s in axial direction. The real shape of combustible zone is compared with CFD numerical simulations in frames of THAI project. It shows rather similar behavior of combustion process in two different scales with different aspect ratios.

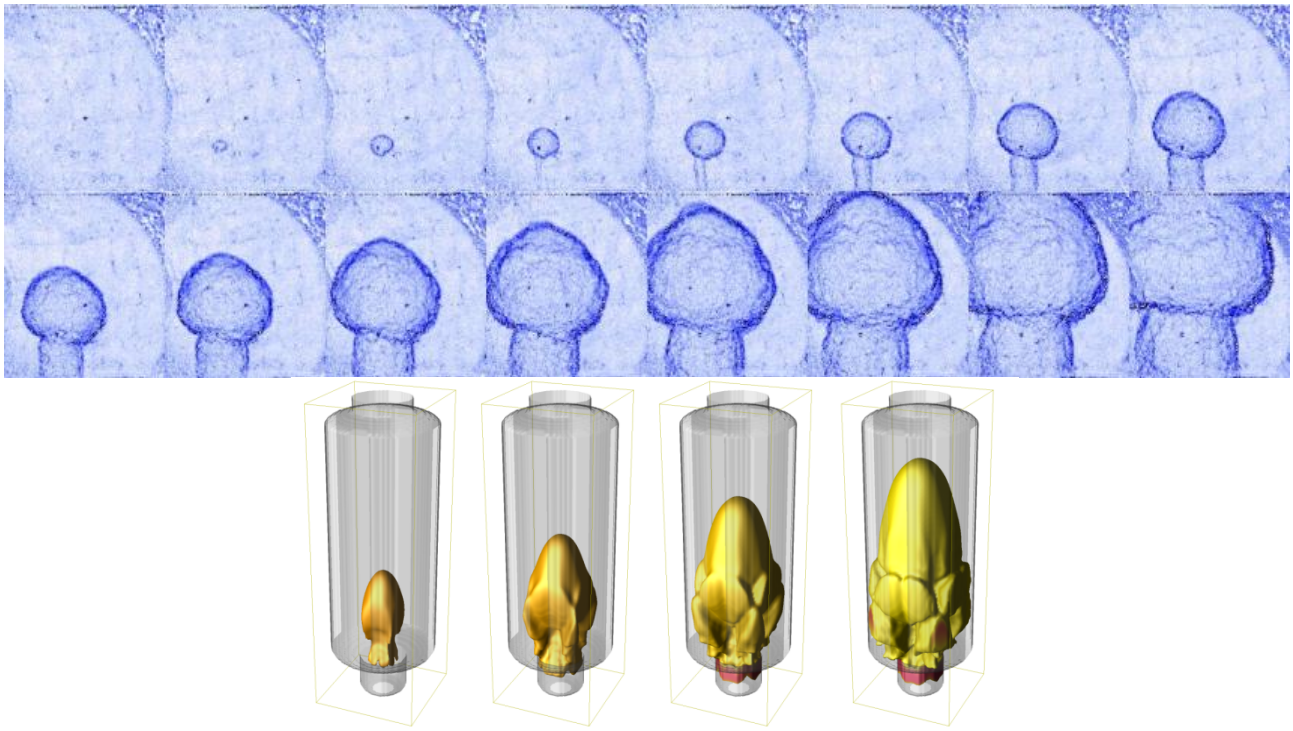

Fig. 32: The sequence of BOS images of the initial flame propagation process in vessel A2 (upper) in comparison with CFD numerical simulations for THAI facility by COM3D-code (lower).

Additionally to video records, detailed measurements of local temperature and pressure were performed in frames of the program. Fig. 33 shows the examples of temperature records for the layers 50, 3000, 4500 and 6000 mm above the floor. Four thermocouples

were radially placed at each layer at the radius 0, 900, 1800 and 2700 mm from the axis. In all figures, the disposition of the start of the temperature increase is consistent with the radial position of the measurement location. The maximum temperature always appears to be reached at the vessel axis. Excluding local peak, which may reach 1200 °C due to the construction effect, the maximum measured temperature was 1018 °C. In comparison with the maximum temperature of 900 – 930 °C observed in the experiment THAI HD-22 in the vessel axis, the maximum temperature observed in the UFPE experiments (excluding fluctuations due to measurement errors) was thus higher for about 100 ºC. The maximum of experimental combustion temperature was well consistent with theoretical calculations of adiabatic combustion temperature of 940 – 980 ºC for isobaric conditions and 1170-1220 ºC for isochoric conditions (Table 11).

Table 11: Thermodynamic properties of test mixtures.

#Test	%H_2 (mol.)	%H2O (mol.)	Initial temp. T_0, K	Initial pressure P_0, bar	Sound speed c_r, m/s	Adiabatic combustion temperature T_{icc}, K	Expansion ratio σ	Adiabatic combustion temperature T_b, K	Adiabatic combustion pressure P_{icc}, bar
HD-22	9.9	25.3	365	1.5	421	1112	2.89	1317	5.14
UFPE01	11.221	20.68	363	1.5	420	1211	3.15	1440	5.62
UFPE02	11.808	20.33	363	1.5	421	1253	3.25	1490	5.79

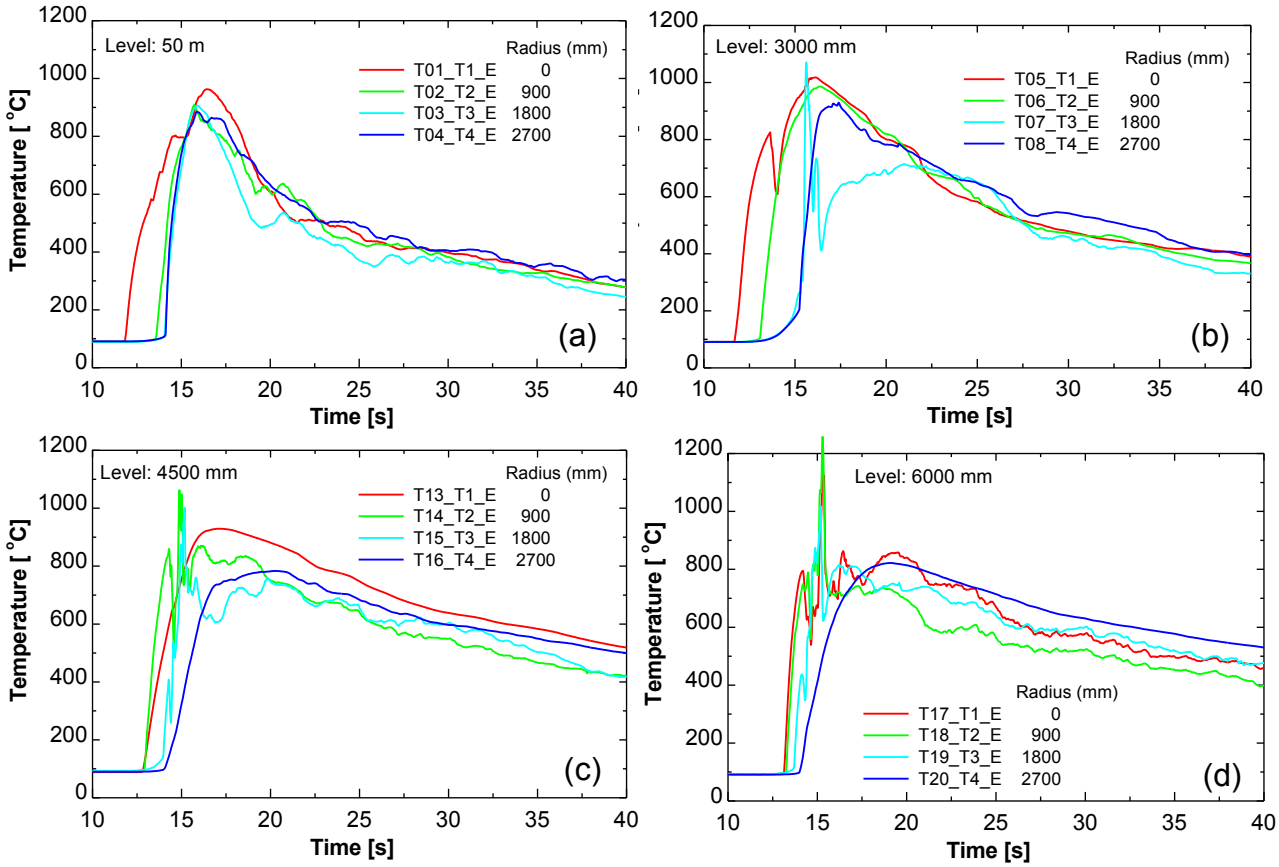

Fig. 33: Temperature records for different layers (a) 50 mm; (b) 3000 mm; (c) 4500 mm; (d) 6000 mm above the floor.

From the flame arrival time based on the temperature measurements it appears that the upward flame velocity was nearly constant, with a value of about 3.1 m/s. For comparison, the flame propagation velocity in the THAI HD-22 experiment was about 2.9 m/s. Thus, these values are very similar. In contrary, the radial (or horizontal) flame velocity at the first elevation above the ignition level is about 0.8 m/s (much lower than the upward flame velocity).

4 Potential impact and the main dissemination activities and exploitation of results

The results of the experiments performed under the LACOMECO project are used for the development of models and their implementation in the severe accident codes such as ASTEC. This will help to capitalise the knowledge obtained in the field of severe accident research in the ASTEC code and the scientific databases, thus preserving and disseminating this knowledge to a large number of current and future end-users throughout Europe. Moreover, the knowledge obtained in the project shall lead to improved severe accident management measures, which are essential for reactor safety and in addition offer competitive advantages for the European industry.

Strong links were established between the LACOMECO and SARNET2 projects, thus improving coordination, pool expertise, and avoiding unnecessary duplication of work:

The results of the LACOMECO experiments are open to SARNET2 partners for joint analysis and interpretation of the experimental results and for code improvements and benchmarking, e.g. the ASTEC code. For example Quench-16 and HYKA UFPE experiments are being used for blind benchmarking of severe accident codes.

Links between the LACOMECO project and PLINIUS severe accident platform of CEA Cadarache were also established. A first joint workshop was held in October 2010 in Aix en Provence (FR).

Furthermore, the results of the LACOMECO experiments were presented and published at different meetings, conferences and in several publications, like:

- LACOMECO session at the annual International Quench Workshop
- Annual ERMSAR conferences
- NENE (Nuclear Energy for New Europe) conference 2010 in Portorož, Slovenia
- NENE ((Nuclear Energy for New Europe) conference 2012 in Ljubljana, Slovenia
- TopSafe 2012 conference in Helsinki
- ISHPMIE-9 (International Symposium of Hazards, Prevention and Mitigation of Industrial Explosions) conference 2012, Cracow, Poland
- ICAPP 2012 (International Congress on Advances in National Power Plants) conference in Chicago, USA
- ICONE-20 (International Conference on Nuclear Engineering) conference 2012 in Anaheim, USA
- ANS Winter Meeting and Nuclear Technology conference 2012 in San Diego, USA
- HEFAT2012 (Heat transfer, fluid mechanics and thermodynamics) conference, Malta

5 Conclusions of the LACOMECO project

The activities within the LACOMECO project allowed advancing considerably towards understanding and perhaps even closure of the most important remaining severe accident safety issues, ranked with high or medium priority by the SARP group for SARNET Network of Excellence. The aim is not only to understand the physical background of severe accidents but to provide the underpinning knowledge that can help to reduce the severity of the consequences. It is crucially important to understand the whole core melt sequences and identify opportunities to lower the risk. This can be done by:

- altering the timing or magnitude of reflooding the degraded core
- in-vessel melt retention in the lower plenum of the RPV
- ensuring the upper bound of system pressure at vessel failure by dedicated depressurisation valves
- Installation of devices or implementing accident management procedures to mitigate melt dispersion into the containment
- Implementation of hydrogen mitigation measures in the containment (ignitors, recombiners etc.)

Main results of the experiments performed in the LACOMECO project are summerised below.

WP1 QUENCH

The QUENCH-16 bundle test with Zircaloy-4 claddings was performed with three typical features before initiation of reflood: moderate pre-oxidation to 135 µm of oxide layer (instead ca. 500 µm for the counterpart test QUENCH-10), a long period of oxygen starvation during the air ingress phase (ca. 800 s instead 80 s for QUENCH-10), and reflood initiation at temperatures significantly below the melting point of the cladding (ca. 1700 K instead of 2200 K for QUENCH-10).

A partial consumption of nitrogen during the oxygen starvation, accompanied by acceleration of the temperature increase at mid bundle elevations, caused the formation of zirconium nitrides inside the oxide layer at bundle elevations between 350 and 850 mm. Due to a noticeable difference between zirconium nitride and zirconium oxide densities, the structure of formed nitride clusters is very porous.

Immediate temperature escalations after reflood initiation, leading to maximum measured temperatures of about 2420 K, were caused by massive steam penetration through the porous oxide/nitride scales and intensive reaction with nitrides and especially with metallic cladding. Very thick oxide sub-layers up to 400 µm were developed during the reflood phase. The cooling phase to the final quench lasted ca. 500 s after achievement of peak temperatures. The total hydrogen production during QUENCH-16 was higher compared to QUENCH-10, i.e., 144 g (QUENCH-10: 53 g), 128 g of which were released during reflood (QUENCH-10: 5 g).

A relatively high concentration of residual nitrides was observed mostly at elevations 350 – 550 mm. Spalled oxide scales with a re-oxidized porous structure were observed at elevations between 350 and 850 mm. 24 g nitrogen from 29 g, consumed during oxygen starvation period, were released during the quench phase. This quantity of released nitrogen corresponds to 7 g (or about 5%) hydrogen developed by re-oxidation of nitrides during reflood. Metallographic investigation of cross sections between 300 and 500 mm showed partially oxidized frozen melt relocated from upper elevations 500 – 800 mm. The melt was formed due to sharp temperature increase on the onset of reflood. The image

analysis of frozen Zr-O melt regions allows estimating the hydrogen release due to melt oxidation to 25 g (or 20% of hydrogen released during reflood).
A significant part of hydrogen (96 g or 75%) released during reflood of the QUENCH-16 bundle was generated due to oxidation of the residual cladding metal layer by steam penetrated through the porous re-oxidized nitride layer.
The consideration of the observed three phenomena (nitriding of α-Zr(O) under oxygen starvation conditions, re-oxidation of nitrides during reflood and accompanying penetration of steam through the porous re-oxidized layer with following oxidation of residual metal, and melt oxidation) should be included in the computer codes to correct prediction of cladding degradation and hydrogen release during reflood of fuel assemblies oxidized under air ingression conditions.

WP2 LIVE

The LIVE-CERAM test provided an original insight into dissolution of refractory material by a volumetrically heated pool. The test results clearly showed that dissolution of solid refractory material can occur in a non-eutectic melt. Dissolution stops when the liquid is saturated in refractory species for the actual interface temperature. Ablation of the refractory layer ultimately stops when the heat flux (delivered by the melt to the refractory) can be evacuated by conduction through the residual thickness of the ceramic, with $T_{interface} = T_{liquidus}$ (actual liquid composition). The final steady state corresponds to a uniform interface temperature distribution. As the pool composition is also uniform in the final steady state (due to convective mixing), the convection in the pool is governed by thermal natural convection and the heat flux distribution is similar to the heat flux distribution that would be obtained for a single component pool.
The LIVE-CERAM results were distributed to SARNET2 WP5-COOL and WP6-MCCI partners for analysis and interpretation.

WP3 DISCO

The DISCO-FCI experiment, devoted to ex-vessel FCI was successfully conducted. The experiment was performed in the DISCO facility (KIT) with a pit geometry close to a French 900 MWe reactor configuration at a scale of 1:10. The fuel was a melt of iron-alumina with a temperature of 2400 K. The nozzle diameter was set to 0.030 m which corresponds to 0.30 m diameter break in reactor scale. There was no hydrogen initially present in the test and the pressure in containment was set to 1 bar of air and 1 bar of vapor. The water level in the pit was about 0.54 m, just below the nozzle, at a temperature of 85 °C.
The containment pressure increased by 0.04 MPa to reach about 0.24 MPa. The pressure in the cavity was characterized by several peaks. The highest peak (0.1 MPa of pressurization, at 0.017 s) cannot be assimilated to a steam explosion. The water inside the cavity (initial 125 kg) has been totally ejected. Concerning the debris, 66% of the initial fuel mass (10.62 kg) remained in the cavity mainly as compact crusts. The fraction of fuel transported respectively to subcompartment and containment were about 10 and 17 %. The size distribution supplied by sieved analysis indicates tendency to small particles with a mean Sauter diameter of 160 µm, a median size diameter of 0.4 mm and a mean mass size diameter of 0.7 mm.
The amount of hydrogen produced by oxidation is about 3% of total moles of gas. The oxidation rates relative to the total mass of Fe and to the dispersed mass are the following:

- Oxidation rate / total Fe mass: 27 % if oxidation to FeO, 18 % if oxidation to Fe_2O_3
- Oxidation rate / dispersed melt: ~ 100 % if FeO, 66 % if Fe_2O_3

This is consistent with the previous DCH tests performed in the DISCO facility. However, the combustion rate is estimated to be 29%. From these results it might be concluded that

the combustion during a FCI, in the absence of pre-existing hydrogen in the containment, has a relatively small impact on the pressurization.

WP4 HYKA (DETHYD)

Critical conditions for steady state detonation propagation were experimentally evaluated in a flat semi-confined layer. The DETHYD experiments were performed in a horizontal semi-confined layer with dimensions of 9x3x0.6 m without obstacles opened from below. The hydrogen concentration in the mixtures with air was varied in the range of 0-34 vol.% with a gradient of 0-1.1 mol. %H_2/cm. Effects of hydrogen concentration gradient, thickness of the layer, average and maximum hydrogen concentration on critical conditions for detonation onset and then propagation were investigated with respect to the safety analysis. Blast wave strength and mechanical response of the safety volume was experimentally measured as well.

The experiments showed that in a semi-open, uniform, stoichiometric hydrogen-air mixture layer the detonation may propagate only if the mixture layer height is greater than approximately 3 cm. This critical value corresponds to the relation with detonation cell size λ as $h^* \approx 3\lambda$. The tests performed with non-uniform hydrogen-air mixture indicated that for hydrogen concentration gradient equal approximately to 1.1 %H_2/cm the detonation may propagate if the maximum hydrogen concentration (near the ceiling) is close to 26 %. Mean detonation layer thickness for this case is equal to approximately 8.5 cm. The lower side of the detonation layer corresponds to hydrogen concentration close to 14 %. For all the experiments, the critical hydrogen concentration for steady-state detonation propagation calculated from the mean values of the detonation layer thicknesses are very similar and close to the 16.6 %. The minimum number of detonation cells (N_{cr} =3-4) in the case of critical layer thickness remains the same as in the case of uniform hydrogen-air mixture. The only common parameter for these experiments is the concentration gradient and it has very strong effect on the detonation decay.

WP4 HYKA (HYGRADE)

Several experiments have been performed in the HYKA test facility to investigate the hydrogen-related phenomena in severe accidents, including hydrogen distribution, hydrogen combustion and hydrogen mitigation measures. Three sets of tests were performed in the facility: a) with initially homogeneous hydrogen gas concentrations, b) with negative gradient initial concentrations, and c) with positive gradient initial concentrations. Positive and negative concentration gradients are created prior to ignition in the range of hydrogen concentrations from 4 % to 13 %, and the process of flame acceleration is investigated depending on hydrogen concentration gradient and ignition positions. Flame time-of-arrival diagrams and pressure evolutions are presented for each test and the results are compared to the data from open literature in terms of potential for flame acceleration-deceleration or even quenching. Explanations are given for a relatively large difference between theoretical AICC overpressures and experimental ones found for some of the tests.

Expansion ratio at the ignition position plays an important role on flame acceleration. In the present case, using the diagram σ_{aver} vs $\sigma_{ign}{*}d\sigma/dx$, fast flames and slow flames are separated by the line $\sigma_{ign}{*}d\sigma/dx = -1.1$. Compared to small scale experiments (TORPEDO, ENACCEF), the quenching phenomena did not occur in large scale in the case of flame propagation in direction of very lean hydrogen concentration.

WP4 HYKA (UFPE)

The Upward Flame Propagation Experiment (UFPE), proposed within the EC LACOMECO project by the Jozef Stefan Institute (Slovenia), was successfully executed at the Karlsruhe Institute of Technology (Germany) in the HYKA A2 facility as planned. The experiment provided valuable results on pressure increase, temperature increase and axial and radial flame propagation, as it complemented and consolidated already existing knowledge based on other experiments. Specifically, the experimental results were compared to the results obtained in the THAI facility, which is of similar height but three times smaller, in the experiment HD-22 that was performed at similar initial conditions. The maximum observed pressure 5.04 bar was similar to the pressure, measured in the THAI HD-22 experiment. This suggests that the wider HYKA A2 facility did not affect the completeness of combustion. The maximum measured temperature 1018 ºC was about 120 ºC higher than the maximum measured in the THAI HD-22 experiment. This suggests that the wider vessel caused an even more intense combustion. However, as the temperature increase is necessarily limited by the heat of combustion and thus by the available hydrogen, no significant further temperature increase is expected in an actual containment. The upward flame propagation velocity (about 3.1 m/s) was similar to the one observed in the THAI HD-22 experiment. In addition, the radial flame propagation velocity (about 0.8 m/s) was estimated to be more than 3 times lower than the upward flame propagation velocity.
The results of the UFPE experiment will be useful for validation of computer codes used in safety analyses, both at the local instantaneous scale (Computational Fluid Dynamics codes) and integral scale (lumped-parameter codes).

The project brought together competent teams from different countries with complementary knowledge. Moreover, the links with the East European research organisations and utilities was established and maintained. Therefore, the project offered a unique opportunity to join networks and activities supporting VVER safety, and for Eastern experts to get access to large-scale experimental facilities in a Western research organisation, thereby improving the understanding of material properties, core behaviour, and containment safety under severe accident conditions.

6 Address of project public website and relevant contact details

http://nuklear-server.nuklear.kit.edu/lacomeco/